THESIS

ASSESSMENT OF THE CLASIC URBAN HYDROLOGY MODEL, IN THE SPRING CREEK WATERSHED, NORTHERN COLORADO

Submitted by

Mahshid Mohammad Zadeh

Department of Civil and Environmental Engineering

In partial fulfillment of the requirements

For the Degree of Master of Science

Colorado State University

Fort Collins, Colorado

Fall 2021

Master's Committee:

Advisor: Mazdak Arabi

Aditi Bhaskar

Michael Ronayne

ABSTRACT

ASSESSMENT OF THE CLASIC URBAN HYDROLOGY MODEL, IN THE SPRING CREEK WATERSHED, NORTHERN COLORADO

Urban development influences the quantity and quality of water at local to watershed scales. Urban hydrology models are commonly used to plan, design, and implement stormwater infrastructure systems to minimize water quality and flooding consequences of urban development. However, the applicability of existing models at municipal scales is hampered by extensive data and computational requirements. The Community-enabled Life-cycle Analysis of Stormwater Infrastructure Costs (CLASIC) tool is a cloud-computing web application that facilitates the simulation of hydrological and water quality responses at municipal scales. The tool also provides modules to assess the lifecycle costs of green stormwater infrastructure systems. CLASIC is a modified version of the EPA's SWMM model with direct linkages to disperse land use, climate, soils, and other data resources.

This study aims to assess the performance validity of the CLASIC tool for the characterization of urban hydrologic processes and responses. Specifically, the objectives of the study are to: i) evaluate the performance of the model compared to the SWMM model and observed stream discharge at various spatial and temporal scales; and ii) identify the most influential model parameters to inform model parameterization. The study is conducted in the Spring Creek catchment within the Cache la Poudre River watershed in Colorado. Streamflow in Spring Creek is influenced by urban activities in the City of Fort Collins. Model evaluation is conducted at hourly, daily, and monthly time steps at two USGS gaging stations along the stream. Comparison of observed and simulated flow duration curves along with several goodness-of-fit measures, including Nash-Sutcliff coefficient of efficiency and percent bias are used to evaluate the model performance. The Sobol' Global Sensitivity Analysis method is used to assess the importance of model parameters for different model responses, including mean and peak stream discharge. The first and total order sensitivity indices are computed to evaluate the effects of parameters individually and in combination.

Overall, hydrological budgets are simulated similarly between CLASIC and SWMM. The results indicate the performance validity of CLASIC stream discharge simulations at computational time steps greater than the time of concentration of the catchment. However, SWMM peak discharge simulations at smaller time steps are closer to the observed behavior of the system. Sensitivity analysis results underline the importance of the Horton infiltration parameters and the percent of imperviousness of the catchment.

ACKNOWLEDGMENTS

I am so grateful for the help and support I have received to complete my degree and research during these two years. I was honored to work with Dr. Mazdak Arabi as my advisor. I would like to express my sincere gratitude to him for his leadership, motivation, and support all the time. I also want to thank my dear committee advisors, Dr. Michael Ronayne and Dr. Aditi Bhaskar, for their help and patience. I would like to thank the National Science Foundation Sustainability Research Network Cooperative Agreement #1444758 for supporting this study.

Finally, I am so thankful to my parents, my sister, and my friends for their love and support during all these years. I would like to thank Tyler Dell, Dr. Ali Tasdighi, and Dr. Mostafa Razzaghmanesh for their help and advice during these two years, as well as everyone in Glover 119. I am so lucky to have a wonderful family and friends like you.

TABLE OF CONTENTS

1. Introduction

Rapid urbanization and growing population have resulted in a significant increase in impervious lands and vegetation removal, altering the natural water balance and threatening the quantity and quality of water resources. Studies have shown that urbanization caused a substantial increase in stormwater runoff and a significant reduction in evapotranspiration (C. Li et al., 2018; Locatelli et al., 2017; Miller et al., 2014). Moreover, the population is growing fast, the rainfall pattern is changing, and the existing infrastructures are aging (Shifflett et al., 2019; Suriya & Mudgal, 2012). Consequently, communities are experiencing severe problems that their conventional infrastructure failed to address, such as increasing flood hazards, property damages, and water quality degradation (McGrane, 2016; Shahed Behrouz et al., 2020; Suriya & Mudgal, 2012). The conventional stormwater infrastructure, also known as Gray Infrastructure, collects the stormwater runoff, conveys it through a piping network, and drains it into water bodies or treatment plants outside the watershed. In contrast, Green Infrastructure mimics the natural water cycle and provides the opportunity for on-site stormwater runoff reduction and treatment (MacMullan & Reich, 2007). The American Society of Civil Engineers (ASCE), in its 2017 Report Card for America's Infrastructure, has declared that investing in upgrading the current stormwater infrastructure is a critical need for the nation's economy and public health (DiLoreto et al., 2020).

The existing problems have triggered municipalities to plan for a shift from their conventional infrastructure to a sustainable infrastructure (e.g., Green Infrastructure); however, they should tackle multiple barriers and challenges. For instance, they are not sure about the performance of green infrastructure, its construction and maintenance costs, or its benefits specifically for their region, with their specific resources and condition (Hammit, 2010).

Therefore, to overcome the barriers, municipalities need a robust tool to help them find the best and most effective alternatives for their current stormwater systems. Nevertheless, modeling urban watersheds and the hydrologic cycle at the municipal scale has been a challenge.

Current models and planning tools have some limitations, such as complexity and need of extensive data to quantify a large number of required parameters (e.g., SWMM), inaccuracy or inability for modeling a large-scale study area (e.g., EPA Storm Water Calculator (SWC)), the limited number of GI practices (e.g., RECARGA), etc. (Dell et al., 2021; Jayasooriya & Ng, 2014). A study in Fort Collins (Dell et al., 2021) was conducted on a large scale study area (2153 acres) that assessed the performance of SWC compared to SWMM. Their study has demonstrated that although the SWC has a reasonable performance in evaluating the average annual hydrologic components (runoff, infiltration, and evaporation) compared to SWMM, it is suggested for smaller study areas up to 50 acres.

The Storm Water Management Model (SWMM) is one of the most popular urban watershed drainage system design and management tools (Haris et al., 2016; Shahed et al., 2020). Many hydrological research studies have been done using SWMM. Jang et al. used the SWMM model to improve the traditional approach of conducting a synthetic hydrograph-urban hydrology model combination for pre- and post-development conditions to model the hydrologic impact of urbanization (Jang et al., 2007). Moreover, the literature shows that SWMM is a reliable tool for flood simulation. An analysis in India was performed in the Brahmani river delta to develop a calibrated SWMM model to predict river floods (Rai et al., 2017). Another study in Urmia city was conducted to find the subcatchments that are most prone to urban flooding during rainy seasons using SWMM (Babaei et al., 2018).

SWMM can also be used to evaluate the performance of Green Infrastructures within an urban area by implementing Low Impact Development (LID) controls. In 2010, LID controls were added to SWMM, including five different generic types (Bio-retention cells, Infiltration Trenches, Continuous Porous Pavement Systems, Rain Barrels (or Cisterns), and Vegetative Swales). Since 2015, this tool has been able to model three more types (Rain Gardens, Green Roofs, and Rooftops) to support managers in planning and designing Green Infrastructures and assessing their effectiveness in runoff reduction (Lewis A. Rossman, 2010, 2015). Many studies have used the SWMM model to evaluate the efficiency of LID controls. For instance, the effect of green roofs in restoring the natural water balance was assessed and compared to impervious roofs using SWMM by Cipolla et al. and Hamouz and Muthanna. Comparing the results between SWMM and the observations illustrated that SWMM has a good performance in simulating runoff from green roofs (Cipolla et al., 2016; Hamouz & Muthanna, 2019). The hydrologic performance of green roofs, porous pavement, vegetative swale, and rain garden compared to a traditional urban development was also evaluated by Kong et al. using the GIS-based SWMM (Kong et al., 2017). Their study has indicated that using LID controls helps to reduce the effect of urbanization on stormwater runoff.

Although SWMM has lots of capabilities, modeling a large-scale watershed with this model requires detailed information about the site-specific parameters and drainage structure that makes a challenge for modelers, especially when there is a lack of data in their study area (Shahed Behrouz et al., 2020).

Community-enabled Lifecycle Analysis of Stormwater Infrastructure Costs tool (Catena Analytics, 2020) is developed as a simplified version of the SWMM model to address the abovementioned issues. CLASIC is a web-based GIS tool funded by the United States

Environmental Protection Agency (EPA) and the Water Research Foundation (WRF), hosted on CSU, eRAMS server, to support stormwater planning and decision making by estimating Lifecycle costs, runoff volume reduction, pollutant removal, economic benefits, social benefits, and environmental benefits. This tool enables users to assess different scenarios of stormwater infrastructure by using different settings and technologies and compare them in terms of their costs and benefits to decide on the extent and combination of green, hybrid green-gray, and gray infrastructure practices (Catena Analytics, 2020). There are ten different types of LID controls, including rain gardens, sand filters, infiltration trench, detention basins, wet ponds, stormwater harvesting, storage vault, permeable pavement, disconnection, and green roof. Each LID type has some default values that are fixed and some input variables that the user can decide on their value. CLASIC needs fewer parameters than a complex model in SWMM since the detailed drainage system is removed and some of the catchment properties are fixed as the default values. Moreover, it populates most of the required data and parameters, such as rainfall and evaporation data, % Land Use, % Imperviousness, slope, soil group, etc., from the national datasets. It also enables users to modify these parameters as desired. It is also worth mentioning that this tool is not intended to be used for flood control (Catena Analytics, 2020; Dell et al., 2021).

To publicly release the CLASIC tool and inform the planners and decision makers about its performance, careful testing of the tool is required to corroborate its reliability and performance validity. This study aims to investigate the reliability of the CLASIC tool for assessing the hydrologic responses compared to a calibrated full SWMM model. It also seeks to identify the important factors in the watershed. Specifically, the objectives are to i) evaluate the performance of the model compared to the SWMM model and the observed stream discharge at various spatial and temporal scales; and ii) identify the most important model parameters to inform model parameterization. This study will inform the decision-makers about the performance of the CLASIC tool in terms of hydrologic responses as a simple tool to evaluate different scenarios and find the best stormwater infrastructure alternatives for their communities.

2. Material and Methods

In this study, we developed a SWMM model using the available data of the Spring Creek watershed and the observed flow data of two gaged locations within the creek. Then a MATLAB code was developed to calibrate the model using 2560 sample sets generated by SIMLAB (method of Sobol) for nine different catchment parameters. Afterward, the CLASIC models were built, and the results were compared to the SWMM model and observed data. An Excel conversion tool is provided to translate the inputs of SWMM into the ones in the CLASIC tool. Moreover, global sensitivity analysis was performed to find the most influential factors of the watershed using the method of Sobol in SIMLAB 2.2.1 and a MATLAB code.

2.1. Study area

Every model is a simplified version of the real world based on assumptions made by the modeler. Calibration is therefore required to estimate the model parameters (Shahed et al., 2020). The Spring Creek watershed in northern Colorado, east of Horsetooth Reservoir, was selected as the study area because there is available observed flow data for this creek.

Spring Creek originates in western Fort Collins, north of Horsetooth Mountain, and after passing through the Horsetooth Reservoir, flows eastward to its confluence with Cache La Poudre River. The Spring Creek watershed (**Figure 1**), which is mainly covered with soil types

B (moderately low runoff potential) and C (moderately high runoff potential) (**Figure 2**), is an urban watershed located in central Fort Collins, Colorado. (**Figure 3**), with an area of about nine square miles, and can be divided into multiple subbasins.

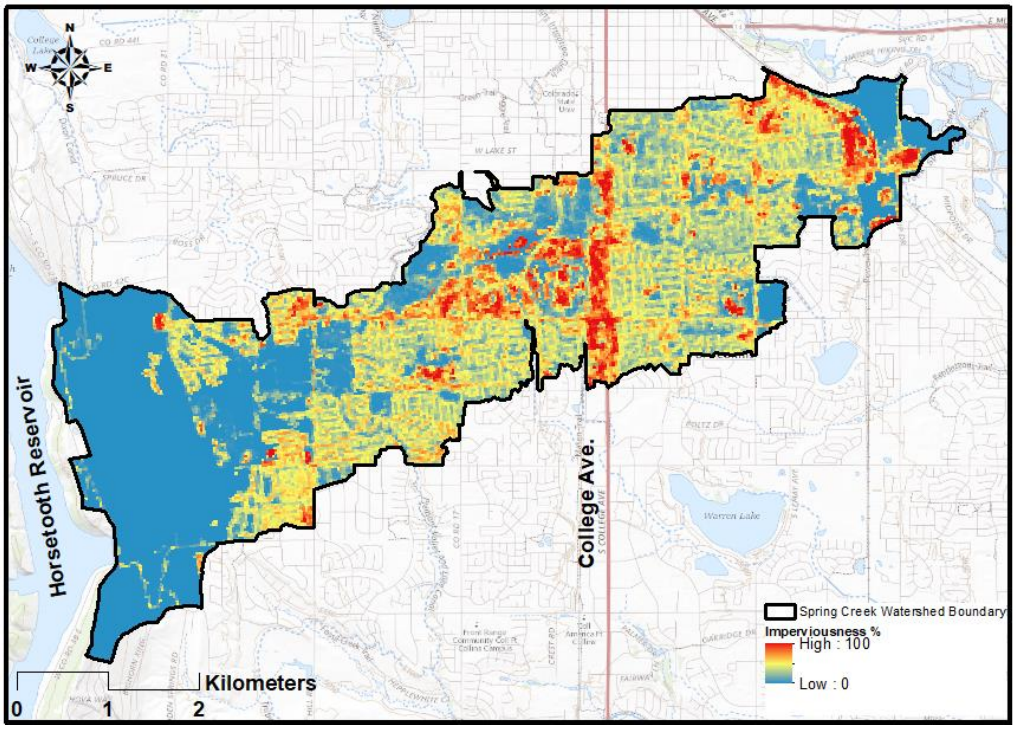

Figure 1: Spring Creek Watershed (Imperviousness Map)

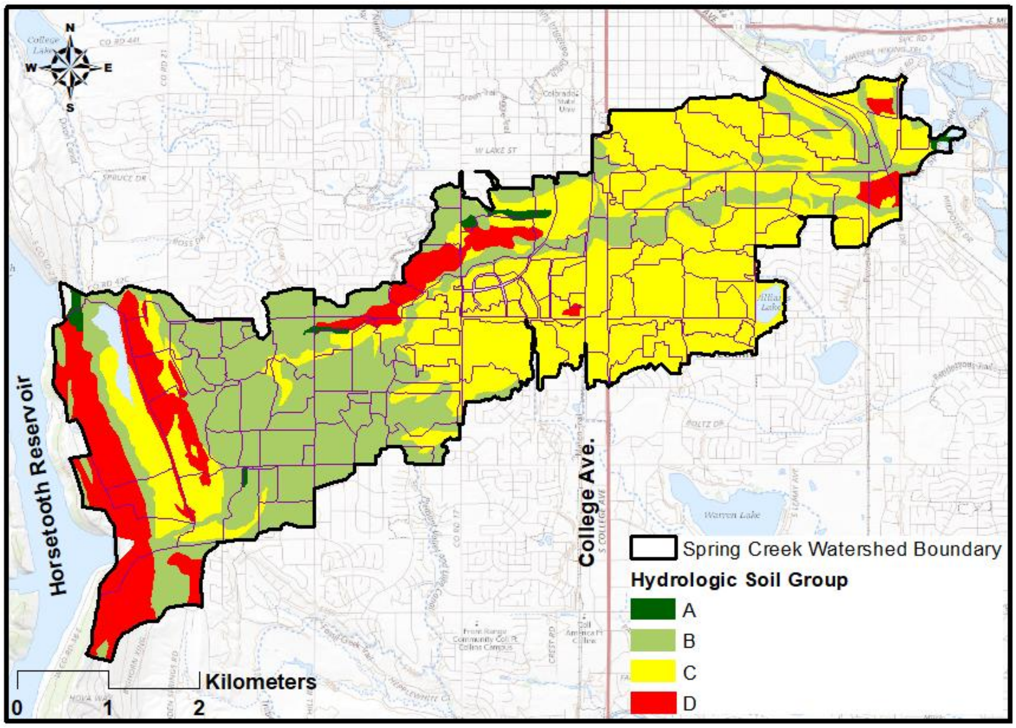

Figure 2: Spring Creek Watershed (Hydrologic Soil Group Map)

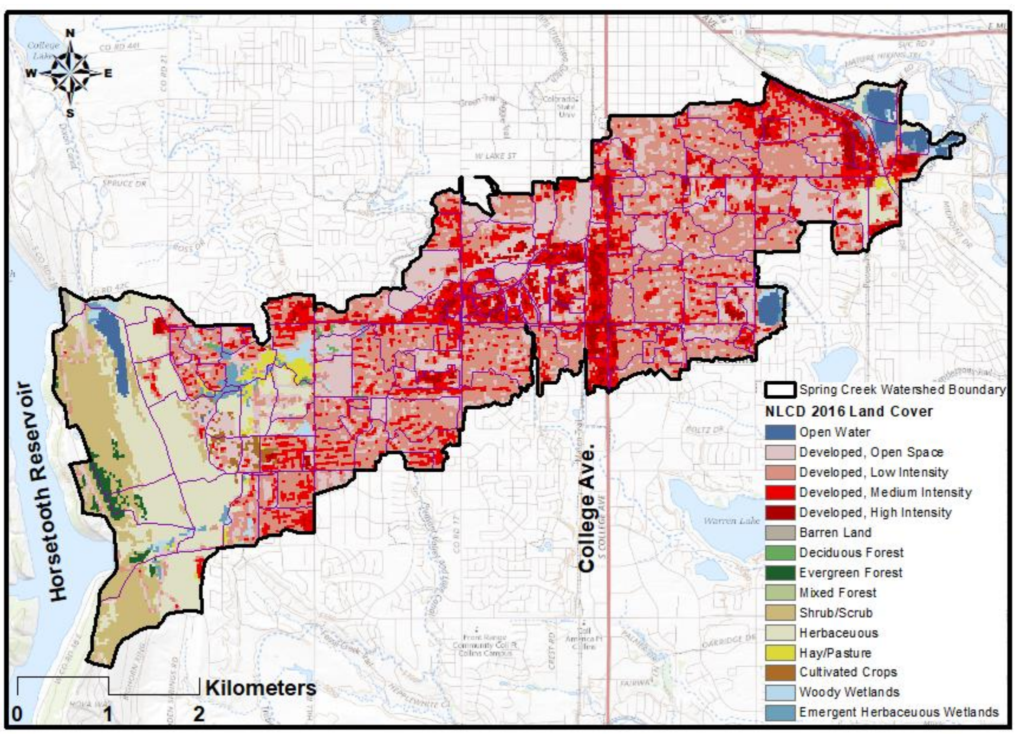

Figure 3: Spring Creek Watershed (Land Cover Map)

2.2. Urban Hydrology Model: Storm Water Management Model (SWMM)

A full SWMM model (SWMM 5.1) for the watershed is built with 134 separate subbasins. Within the watershed, there are two gauged locations where the hourly observed flow values from 2000 to 2018 are collected. These two locations are the intersections of the creek with Center Ave. and with Timberline Rd. (**Figure 4**). The required data of each subbasin and the drainage network were collected from the City of Fort Collins dataset and the Google Earth measuring tool. The City of Fort Collins provided the input and output files of an old version of the SWMM model for the Spring Creek watershed. This model was first developed by the University of Florida in 1970 and then updated in 1973, 1974, 1985, and 2003 by the University of Florida, Missouri River Division, Boyle Engineering Corporation, and Anderson Consulting Engineers, respectively. SWMM96 (Watson, 1996) was used to build the old version, and there are some differences in the modeling approach and notations between this version and the recent versions. For instance, there is no invert elevation of nodes reported in the old version file; instead, it has the invert slope of each conduit. Invert elevation of a node is the elevation of the bottom of a manhole or the joint of two conduits. To address this issue, the approach was to start from the outlet's surface elevation and subtract the maximum depth of the conduit at that point from this elevation. Then, calculate an invert elevation for each upper node using the slope of the conduits.

Another difference between these two versions is how they represent the storage unit properties. In the old version, the approach is to enter the total storage volume of the storage unit versus the spillway outflow; however, in the new version, it is done by creating storage curves to represent the cross-section of the storage unit based on depth versus area of different levels, and rating curves to represent head versus outflow. Since there was no data available for the cross-section of the storage units, they are assumed to be rectangular. The surface area of each storage unit was extracted from the GIS shapefiles provided by the City of Fort Collins and the Google Earth measuring tool. Then their depth was calculated by dividing the volume by the surface area. Moreover, some additional storage units were added to the old model based on the current maps.

There are also some other differences between the old and recent versions related to routing models. Dynamic Wave routing model is selected for the SWMM model in this study since it accounts for different phenomena such as backwater effects, flow reversals, pressurized flow, and entrance/exit energy losses (L.A. Rossman, 2006).

The selected settings for this model are the Dynamic Wave routing model, Horton infiltration method, and continuous simulation. Horton infiltration (Horton, 1941) is a well-known method to calculate the infiltration capacity of the soil. Based on this approach, infiltration capacity decreases during a long rainfall event. It starts from a maximum infiltration rate and decreases exponentially to a minimum rate, with a specific decay rate (James & Rossman, 2003).

The drainage system is a complex network including 144 junctions and an outfall node, 185 conduits consisting of pipes and channels, and 48 storage units representing the detention and retention ponds and their outlet links (**Figure 5**). The drainage network collects the runoff of each subbasin that is drained to the assigned node, then conveys the water through the conduits and drains to the Spring Creek on its path to the outfall node.

To perform a continuous simulation, we need to use long-term precipitation and monthly evaporation data. National Stormwater Calculator (SWC) and CoAgMET are used to collect monthly evaporation and hourly precipitation data (2006-2018), respectively. The first nine years of the precipitation data (2006-2014) are used for calibration, and the first two years of this period are considered as the model's warm-up period. Furthermore, the last four years of the precipitation data are used to test the calibrated model's performance. Furthermore, SSURGO data (Soil Survey Staff, 2019) is used to identify the soil characteristics beneath the storage units. Baseflow is also extracted using the WHAT baseflow separation tool and added to the models (Lim et al., 2006).

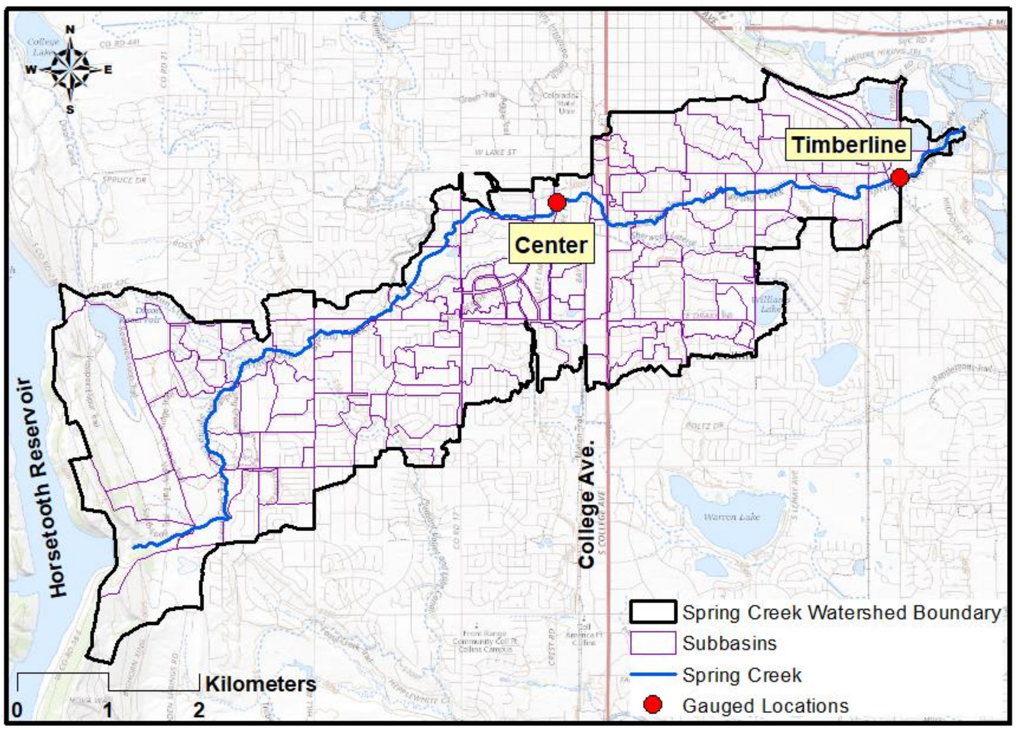

Figure 4: Spring Creek Watershed

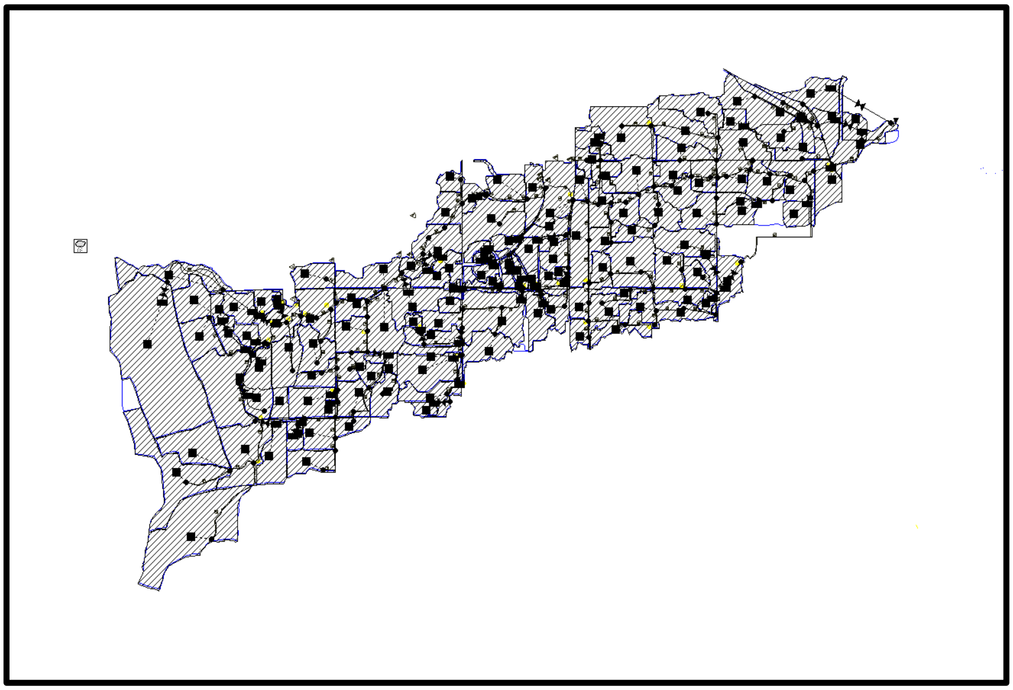

Figure 5: Spring Creek Watershed SWMM Model

2.3. Sensitivity Analysis and Calibration

Hydrological models are merely simplified representation of the real-world phenomena and resolve hydrologic processes responses at discrete spatial and temporal scales. Thus, discrepancies between model predictions and observations are unavoidable. Various sources of uncertainty in hydrological modeling include (Beven, 2001; Renard et al., 2010; Song et al., 2015; Tasdighi et al., 2018; Vrugt, 2016):

- Input uncertainty: This kind of uncertainty is related to the inaccurate forcing inputs while collecting data or initial conditions (e.g., precipitation data).

- Structural uncertainty (model uncertainty): This source of uncertainty results from simplifying the model and processes in the model, errors in the methods used, and/or the lack of information.
- Parameter uncertainty: The lack of knowledge about some parameters or inability to find their exact value would cause this type of uncertainty in the model.
- Measurement uncertainty: The uncertainty related to the measurement of observed data (e.g., discharge data).

Sensitivity Analysis (SA) is used to determine how model outputs are influenced by the uncertainty of input factors, and it plays an essential role in any hydrological research. There are different techniques for sensitivity analysis, such as Global SA, Local SA, and screening SA, and each of them has different methods.

Local SA is the simplest approach type of sensitivity analysis, which considers a small local range of each input factor, one at a time, around its base point. Thus, in this approach, a meaningful initial value for the uncertain input factor is needed (Pianosi et al., 2016). This technique is computationally cheap to implement but has some shortcomings, such as its dependence on the size of the perturbation and the basepoint in nonlinear models and inability to account for parameter interactions (i.e., one parameter depends on the value of another parameter) (A. Saltelli, 1999; Song et al., 2015). This method was used widely as a pre-calibration sensitivity method to reduce the number of factors in calibration, as it is reviewed by Shahed Behrouz et al. (Shahed Behrouz et al., 2020).

Screening method, proposed by Morris in 1991, is based on the elementary effects to show the overall effect of each input on the output (Morris, 1991). In this method, the elementary effects are calculated for each input, then their average (μ) and standard deviation (σ) are computed as sensitivity measures. A higher mean value indicates that the input factor has a more overall influence on the output, and a high standard deviation shows non-linearity or interaction between the input factor to other input factors (Campolongo et al., 2007; Wagener, 2013). This approach is suitable to lower computational costs for the models with a high number of uncertain parameters compared to global SA methods. However, not accounting for the interactions between parameters, the effect of different inputs on the output at a time, and self-verification are some of the weaknesses of this method (Campolongo et al., 2007; Song et al., 2015).

Global SA technique explores the whole feasible range of the uncertain parameter and evaluates the interactions between the parameters. Based on Saltelli et al.'s studies, the global method is more reliable than the Local method when Error type II (acceptance of a false null hypothesis) is important, and it is suitable for nonlinear and non-monotonic models (A. Saltelli et al., 2008; Song et al., 2015). According to Song et al. (2015), some of the commonly used global SA techniques in hydrologic modeling are the Regressive-based method, Variance-based method, Metamodeling-based method, RSA, and Entropy method. In their work, the main studies of global sensitivity analysis in hydrological models since 2005 are reviewed, and it is concluded that variance-based methods are of more interest than other methods of global SA techniques (Song et al., 2015). Variance-based methods are robust model-independent methods that aim to evaluate the sensitivity of the output variance to the uncertainty of the inputs and interactions between them, assuming that the variance is sufficient to assess the uncertainties and sensitivities. However, the drawback of this approach is its computational cost, which led researchers to make the process more efficient (Baroni & Francke, 2020; Giap & Kosuke, 2014; Khorashadi et al., 2017; K. C. A. Saltelli & Tarantola, 1997).

Considering the wide range of advantages and capabilities of global sensitivity analysis compared to other sensitivity approaches, modelers have used this method for many different purposes in hydrological and hydraulic modeling (J. Li et al., 2013; Nossent et al., 2011; Pfannerstill et al., 2015; Sanadhya et al., 2014). Therefore, in this study, the method of Sobol is used, which is one of the variance-based methods.

2.3.1. Method of Sobol Global Sensitivity Analysis

The method of Sobol, named after a Russian mathematician Ilya M. Sobol, was developed in 1990 based on the Fourier Haar series (1969) for nonlinear models. Sobol used Monte Carlo methods to evaluate multidimensional integrals to estimate sensitivity measures (Archer et al., 1997). These integrals are used to calculate all terms of the decomposition of the output function $f(x)$ (K. C. A. Saltelli & Tarantola, 1997; Andrea Saltelli et al., 2010):

$$Y = f(x_1, \dots x_n) = f_0 + \sum_{i=1}^{n} f_i(x_i) + \sum_{i=1}^{n} \sum_{j=i+1}^{n} f_{ij}(x_i, x_j) + \cdots + f_{1,2,\dots,n}(x_1, \dots x_n); \; (x_m \in K^n) \tag{1}$$

Then, by squaring and integrating (1) over K^n and considering that all the summands in (1) are orthogonal, the decomposition of the output variance would be obtained:

$$V = \sum_{i=1}^{n} V_i + \sum_{i=1}^{n} \sum_{j=i+1}^{n} V_{ij} + \cdots + V_{1,2,3,\dots,n} \tag{2}$$

Afterward, by dividing partial variances of each term in (1) by the total output variance, first-order sensitivity measures will be calculated:

$$S_i = \frac{V_i}{V(Y)} = \frac{V_{x_i}\left(E_{x\sim i}(Y|x_i)\right)}{V(Y)} \tag{3}$$

The FAST method could be used instead of Sobol if the sum of the V_i terms were close to the total output variance. Otherwise, higher order indices—that are, the interactions between the selected factor and other factors—need to be calculated to allow the investigator to find the total effect index (S_i^T) of each parameter (x_i) on the output variance in addition to the main effect. (A. Saltelli & Homma, 1996)

S_i^T would be the sum of all terms, including the subscript i (A. Saltelli et al., 2012). As an example, if we consider only three input factors, then S_i^T would be defined as follow:

$$S_i^T = S_i + S_{ij} + S_{ik} + S_{ijk} \tag{4}$$

When Sij and Sijk are the second-order and third-order indices, respectively.

The smallest sample size in this method is n(2k+2). The term "n" is the minimum model evaluation for estimating one individual effect, taking a value of 16, or 32, 64, 128,…, and the term k is the number of input factors (Koo et al., 2020; Nguyen & Reiter, 2015; A. Saltelli, 2014).

The main drawback of the Sobol method is that it is computationally expensive and time-consuming, and its main advantage is that one can estimate the sensitivity of any order with this method. Furthermore, the application of this method is suitable for nonlinear, non-monotonic models and can be considered as a quantitative, model-independent approach. (Andraddttir et al., 1997;Becker, 2014)

This method is widely used in hydrologic and environmental models. Studies have found the method of Sobol very successful in factor fixing and factor prioritization for flow simulations

(Cibin et al., 2014; Nossent et al., 2011). Leimgruber et al. also found this method proper to evaluate the sensitivity of water balance components to LID parameters using a SWMM model (Leimgruber et al., 2018).

To perform global sensitivity analysis on the SWMM model, SIMLAB 2.2.1 is used to generate 2560 sample sets for nine independent parameters with the method of Sobol (**Table 1**). The parameters are width of the subbasins, slope of the subbasins, percent of imperviousness, depression storage in impervious and pervious area, the percent of impervious area without depression storage, and Horton infiltration parameters. A range of fractions (scale factors) is selected for each parameter based on the parameters' feasible range (Dell et al., 2021; Lewis A. Rossman, 2015). To simplify the process, each parameter would have the same scale factor for all the subbasins in each sample set. It is assumed that all parameters are uniformly distributed so that for each parameter, there is the same probability of having any value within its feasible range. Since estimating the indices of all orders is very expensive in the method of Sobol, it is customary to estimate only first and total order indices (A. Saltelli et al., 2010).

Table 1: Range of parameters for sensitivity analysis in SIMLAB

Parameter	unit	Lower bound	Upper bound	Lower bound fraction(unitless)	Upper bound fraction(unitless)
Width	ft	350	20820	0.7	1.2
Slope	%	0.25	43.8	0.5	2
%Imperv	%	4	99.9	0.5	1
DstoreImperv	in	0	0.1	0	1
DstorePerv	in	0.1	0.3	0.33	1
%ZeroImperv	%	1	5	1	5
Max Infil Rate	in/hr	1	10	1	19.6
Min Infil Rate	in/hr	0.01	0.5	0.02	1
Decay Rate	1/hr	2	13	0.3	2

Afterward, a MATLAB code is developed to run the model in SWMM for each sample set and generate the flow at both gauged locations (i.e., intersections of Spring Creek with Center Ave. and Timberline Rd.). Each sample set of parameters is the product of the selected parameters and their respective generated scale factor from SIMLAB for that parameter.

After running all sample sets in SWMM, the simulated flow for each set and location is compared to the available observed flow to find the best sample set by evaluating the model performance metrics. Statistical model performance metrics that are evaluated for this study are Coefficient of determination (R^2), Root Mean Square Error (RMSE), Nash-Sutcliffe coefficient of efficiency (NSE), and PBIAS. **Table 2** shows the formula to calculate each metric (Moriasi et al., 2015). N is the number of samples, S_i is the simulated flow and O_i is the observed flow.

Table 2: Model performance Metrics (statistical)

Equation	Range	Best value
$R^2 = Corr^2(S, O)$	0 to1	1
$RMSE = \sqrt{\frac{\sum_{i=1}^{N}(O_i - S_i)^2}{N}}$	0 to ∞	0
$NSCE = 1 - \frac{\sum_{i=1}^{N}(O_i - S_i)^2}{\sum_{i=1}^{N}(O_i - \bar{O}_i)^2}$	-∞ to 1	1
$PBIAS = \frac{\sum_{i=1}^{N}(O_i - S_i)}{\sum_{i=1}^{N}(O_i)} \times 100$	-∞ to ∞	0

Each metric has some advantages and disadvantages discussed by Moriasi et al. (Moriasi et al., 2015). The objective of the calibration process was to find the parameter set with the best

NSE value. Moreover, it is recommended to use a combination of statistical and graphical performance measures to understand the model's performance better (Loague & Green, 1991; Moriasi et al., 2015). Hence, this study selected time series, 1:1 scatter plot, Cumulative distribution curves (CDF), and Flow Duration curves (FDC) as the graphical measures. As one of the most commonly used graphical measures in hydrology, Flow Duration Curve represents the percent of the time a given flow is equaled or exceeded (Vogel & Fennessey, 1996). Many studies related to hydrology, water quality, watershed management, flood assessment, etc., have considered FDC a useful means (Leong & Yokoo, 2021). For example, Brown et al. found FDC helpful in evaluating the impact of vegetation change on flow distribution (Brown et al., 2005). FDC has also been used extensively in predicting streamflow in ungagged locations (Burgan & Aksoy, 2018, 2020; Müller & Thompson, 2016). Moreover, this curve can be an alternative to CDF curves (Leong & Yokoo, 2021), but both are presented in this study.

Sensitivity indices for total effect and main effect are generated using SIMLAB by performing global sensitivity analysis with the method of Sobol for Average Annual flow, Standard Deviation (SD) of Annual flow, Average Annual Peak flow, and SD of Annual Peak flow.

2.4. CLASIC model

CLASIC tool uses a simplified methodology to route stormwater with and without Low Impact Development technologies called SWMM-LITE (Dell et al., 2021). After calibrating the SWMM model, three models were built in the CLASIC tool. Building a model in the CLASIC tool requires fewer parameters than the SWMM model. There is no need to have the drainage system parameters, or some parameters related to the subbasins such as manning N for the impervious and pervious area, depression storage of impervious and pervious area, and percent of the impervious area without depression storage. CLASIC models each subbasin (with or without LID) separately and drains its runoff to a separate conduit. Then, all conduits drain into the outfall. Thus, to get the flow of each channel in the watershed, we need to model the upstream drainage area of that channel so that the outfall node of the model would represent the upstream node of the channel in the watershed. Since we have two gauged locations, two models were created to simulate the flow of these two locations. One model is the upstream drainage area of Center Ave. gauge (**Figure 7**), and the second model is the upstream drainage area of Timberline Rd. gauge (**Figure 8**). Another model (**Figure 6**) is also built for the entire watershed to simulate the hydrologic components of the study area (Runoff, Evaporation, and Infiltration). To build each model, the shapefile of the desired drainage area is imported into the tool as the project area. Then, the precipitation and evaporation data are entered in the Climate Data tab. Afterward, the properties of the subbasins are applied to them separately. At this point, the baseline scenario is built (a scenario without any LID controls). By creating a new scenario, we can build our final model with LID controls. Since only the data of Detention ponds and Retention ponds were available for this watershed, they are the only LID controls considered in this study.

Considering the differences between the model that can be built in the CLASIC tool and the model already built in the SWMM, a conversion tool is provided to translate the storage units from SWMM into the LID controls in the CLASIC tool (**Figure 9**). This tool is a spreadsheet that summarizes the main factors of the drainage area and LID controls (or storage units) for each subbasin and calculates the number of the converted technologies needed in the CLASIC tool to maintain the main factors. The most similar technology to what we have on the site should be selected in the conversion process, and the main factors should be kept consistent. The main factors are total drainage area, total technology area, total captured volume, seepage rate, and total % of imperviousness. Since detention ponds and retention ponds are volume-based technologies, the most important factor in the CLASIC models is the total captured volume (Dell et al., 2021).

Time of concentration (T_C) at each gauged location is also evaluated by the SCS method. T_C is the time that runoff needs to reach the outlet from the hydraulically furthest point of the watershed (USDA-NRCS, 2010). The SCS method uses curve number (CN) and the catchment characteristics to evaluate the time of concentration:

$$T_C = \frac{L^{0.8}(S+1)^{0.7}}{1140Y^{0.5}} \tag{5}$$

Where:

T_C = time of concentration (hr)

L= flow length (ft)

S= maximum potential retention (in) (S = $\frac{1000}{CN} - 10$)

Y= average watershed land slope (%)

The selected average value of 80 as the curve number (CN) is determined based on the watershed land cover and soil group (NEH630.09, 2004).

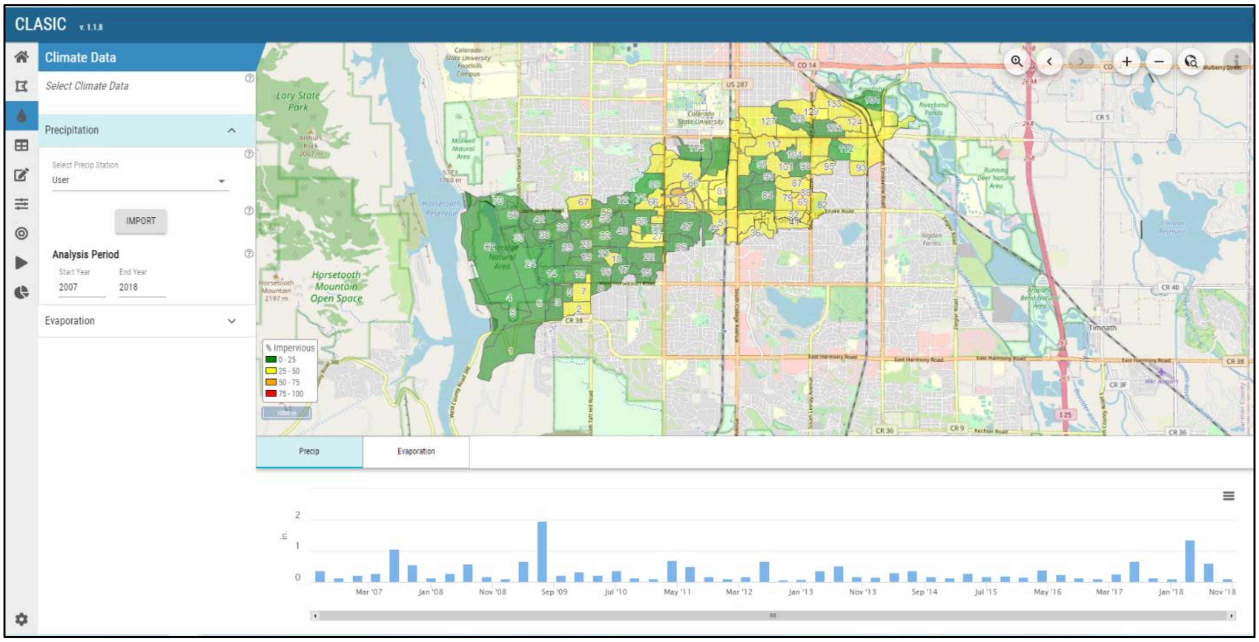

Figure 6: CLASIC model for the entire watershed

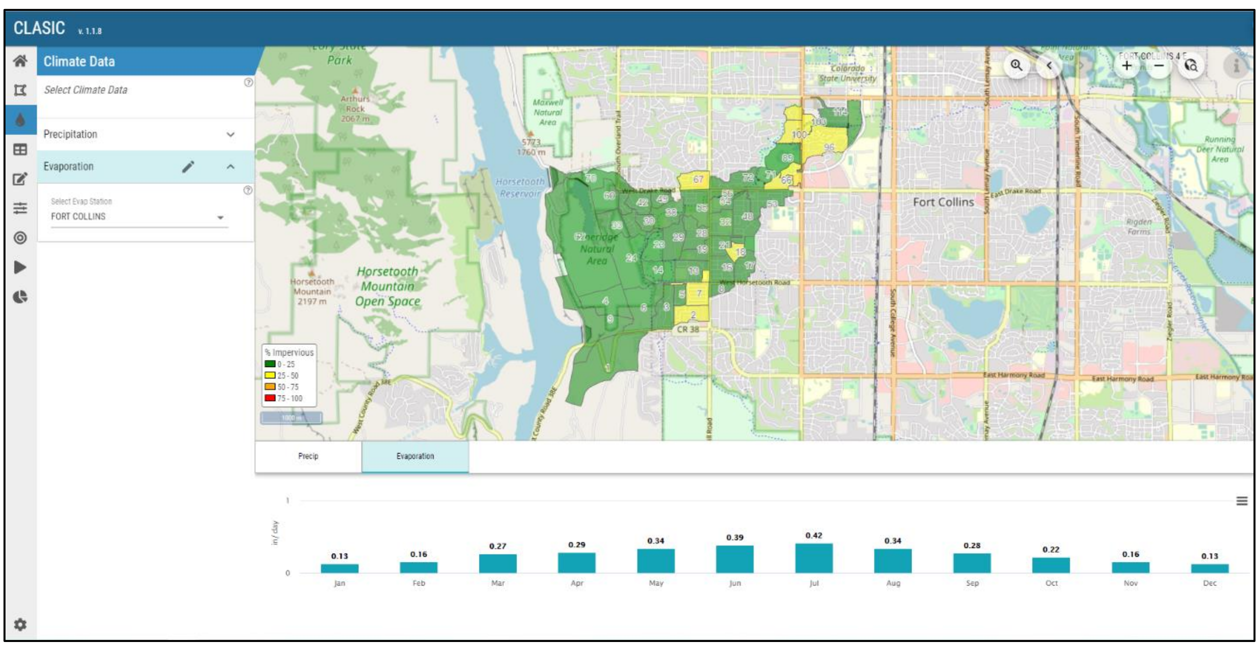

Figure 7: CLASIC model for Center location

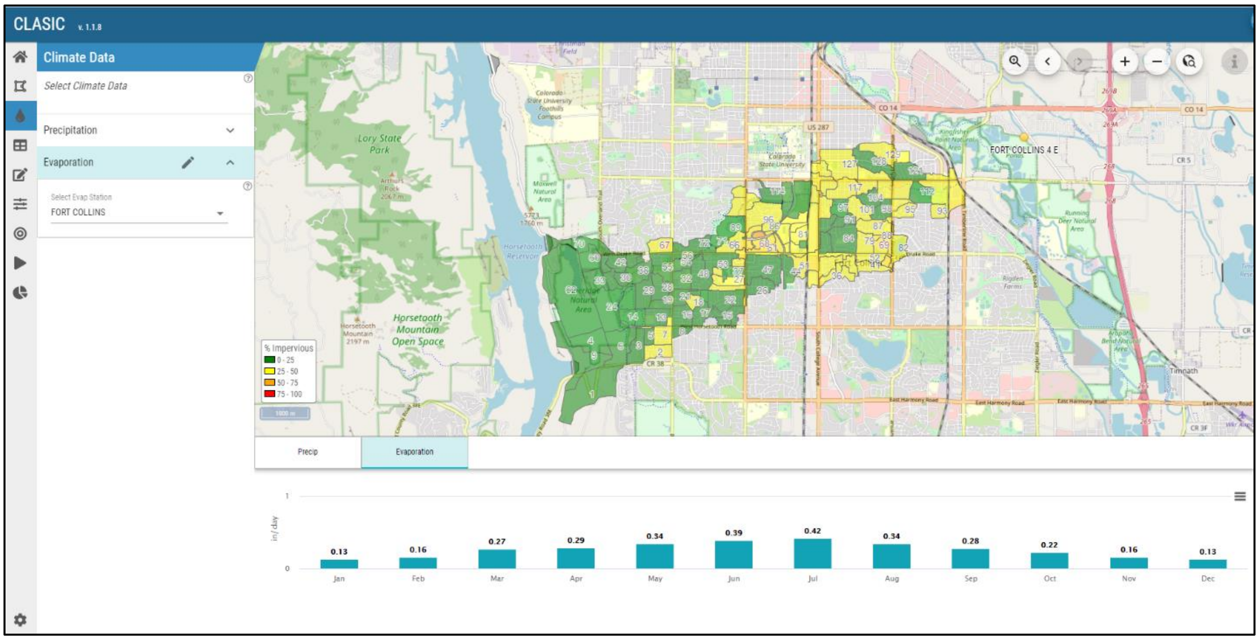

Figure 8: CLASIC model for Timberline location

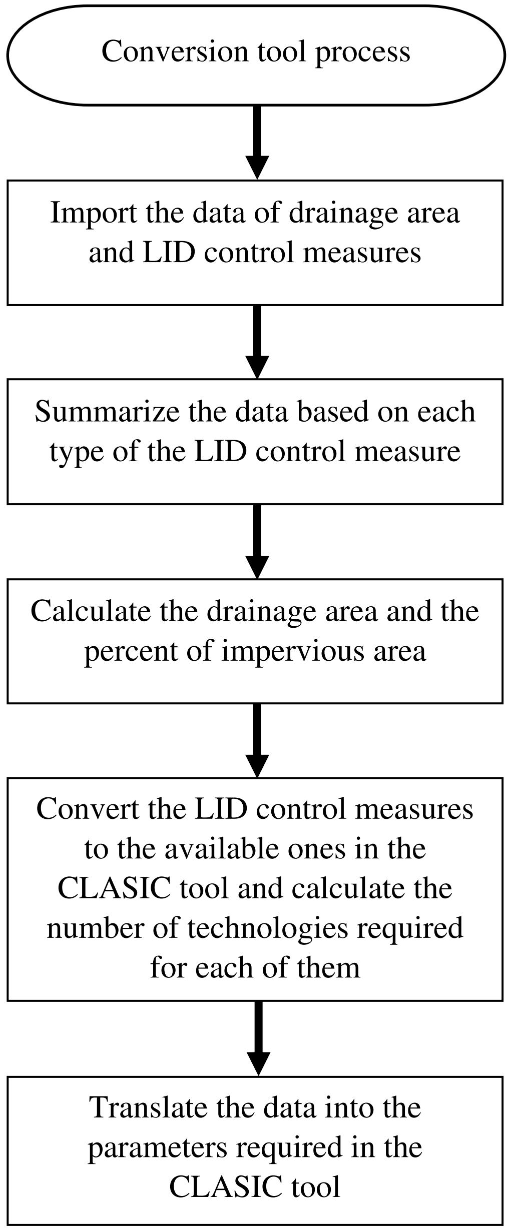

Figure 9: Conversion tool flowchart

3. Results

3.1. SWMM Calibration and testing

The SWMM model was calibrated against observed flow data at two locations (Center and Timberline) for 2008 through 2014 using feasible ranges of catchment parameters (**Table 1**). A parameter set with the closest NSE to one is selected as the best set for the model, while other performance metrics are also tested to be acceptable (**Table 3**). The selected set of fractions is 0.7273 for width, 1.9414 for slope, 0.5039 for percent of impervious, 0.7890 for depression storage of impervious area (DstoreImperv), 0.76445 for depression storage of pervious area (DstorePerv), 2.78125 for percent impervious area with no depression storage (%ZeroImperv), 13.0609 for max infiltration rate, 0.76265 for min infiltration rate, and 0.6320 for decay rate. The model is then tested for another period (2015-2018), and the results are shown in **Table 4**.

Based on the performance evaluation criteria by Moriasi et al. for a watershed scale model, NSE>0.8, R^2>0.85, and PBIAS<±5 show "Very Good" performance for daily and monthly temporal scale (Moriasi et al., 2015). Their study also found that 0.7< NSE ≤0.8, 0.75< R^2 ≤0.85, ±5≤PBIAS≤10 represent "Good" performance. **Table 3** shows that the calibrated model has a very good performance based on NSE and R^2 in the calibration period (2008-2014) in both observed locations. PBIAS in Center location for all temporal scales has a "Good" rating while in Timberline location has a "Very Good" rating. Moreover, Singh et al. recommended that the RMSE value less than the standard deviation (SD) of the observations be considered low (Moriasi et al., 2015; Singh et al., 2005). SD for hourly, daily, and monthly observation flows are 25.53, 19.62, and 16.8 (CFS) in the Center location and 21.78, 12.59, and 10.14 (CFS) in Timberline location, respectively. Thus, the results in **Table 3** indicate that RMSE values are low for all the temporal scales, and in both locations, that is very good.

As mentioned above, **Table 4** shows the model's performance in a period other than the calibration period. This table shows that PBIAS has a "Good" rating, and NSE and R^2 have a "Very Good" rating for all temporal scales and locations. Furthermore, SD for hourly, daily, and monthly observed flow equals 14.64, 10.75, 9.64 in the Center location, and 19.32, 13.37, and 10.79 in Timberline location, respectively. Based on the SD values and **Table 4**, the SWMM model also has low RMSE in this period of time.

Table 3: Model performance metrics (2008-2014)

Location		**PBIAS (%)**	**RMSE (CFS)**	R^2	**NSE**
Center	Hourly	8.7	9.8	0.87	0.85
	Daily	7.22	5.33	0.94	0.93
	Monthly	8.15	3.77	0.98	0.95
Timberline	Hourly	-0.06	11.99	0.86	0.70
	Daily	4.95	5.51	0.89	0.81
	Monthly	1.22	2.52	0.95	0.94

Table 4: Model performance metrics (2015-2018)

Location		**PBIAS (%)**	**RMSE (CFS)**	R^2	**NSE**
Center	Hourly	9.03	4.9	0.90	0.89
	Daily	8.30	2.52	0.96	0.94
	Monthly	8.80	1.79	0.99	0.96
Timberline	Hourly	6.51	7.98	0.87	0.83
	Daily	8.10	3.91	0.92	0.91
	Monthly	9.74	2.66	0.95	0.94

To get a visual indication of the model performance, graphical performance measures are also provided in **Figures 10 to 17** for the calibration period and **Figures 18 to 25** for 2015-2018. **Figure 10** and **Figure 11** show the time series of observed and simulated flows for different temporal scales in the Center and Timberline locations, respectively, for the calibration period. These figures show that the model could capture the shape and peak time of the observed flow very well in both locations. However, there are some locations in the time series that the model has underestimated or overestimated the peak flow. In the Center location, the SWMM model mostly underestimated the peak flow, while the model mostly overestimated the peak flow in the Timberline location.

There is a significant peak flow in both time series of gauged locations due to a large precipitation event in July 2009. The time series show that the SWMM model couldn’t evaluate the actual magnitude of that event; hence it has caused overestimation of flow at both locations. Moreover, as the computational time scale gets bigger, the difference between observed and simulated peak flows becomes smaller.

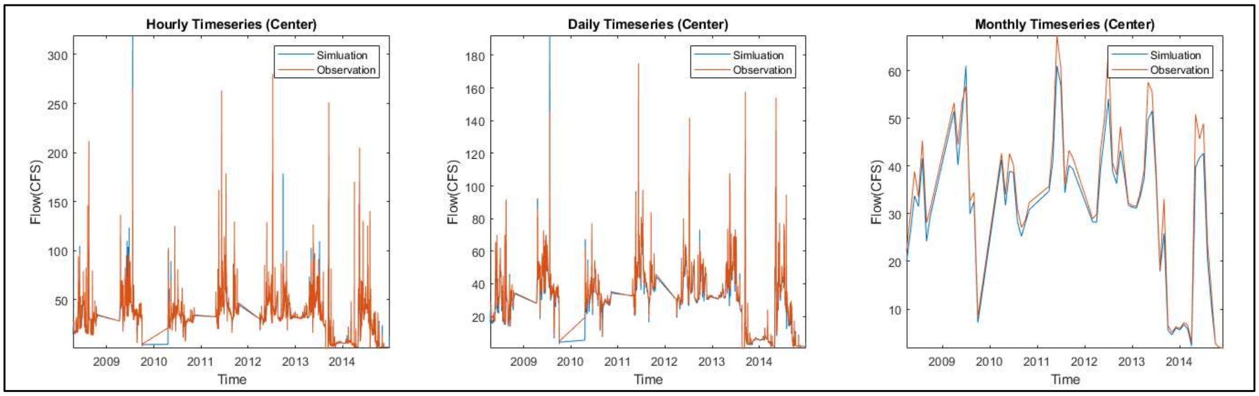

Figure 10: Timeseries of observed and simulated flow in Center (2008-2014)

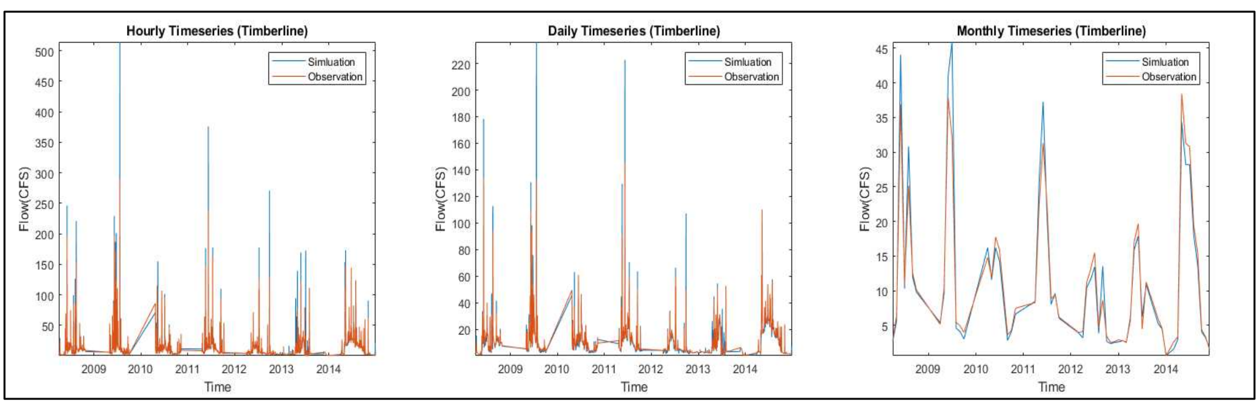

Figure 11: Timeseries of observed and simulated flow in Timberline (2008-2014)

Figure 12 and **Figure 13** show the scatter plots of observed flow versus simulated flow for different temporal scales in Center and Timberline locations, respectively, for the calibration period. These figures show that the model mostly underestimated the flow in the Center location, while it mostly overestimated the flow in the Timberline location. These plots also show that the points are more scattered with more distance from the 1:1 line in a smaller time scale, and they get closer to the line as the temporal scale gets larger.

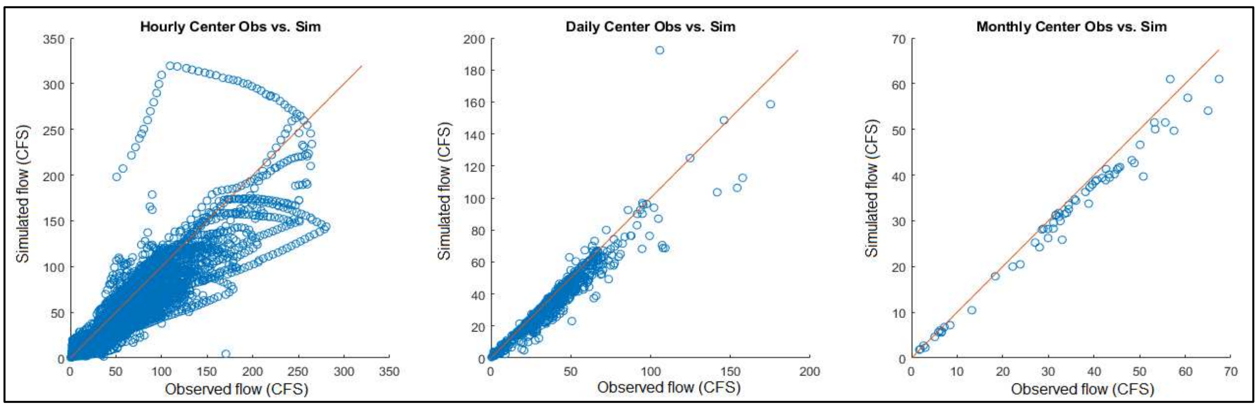

Figure 12: Scatter Plot of simulated vs observed flow at Center (2008-2014)

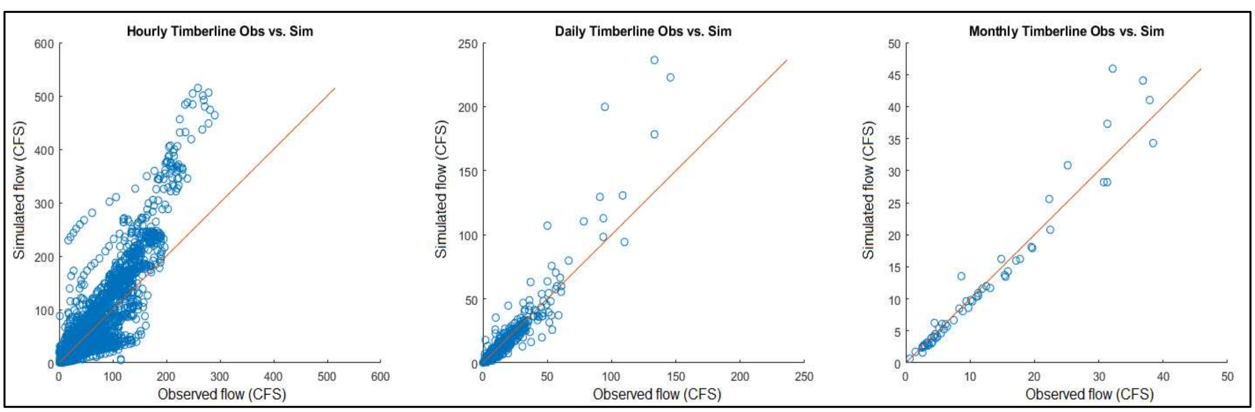

Figure 13: Scatter Plot of simulated vs observed flow at Timberline (2008-2014)

Figure 14 and **Figure 15** show the Cumulative Distribution Function (CDF) curves of observed flow and simulated flow for different temporal scales in Center and Timberline locations, respectively, for the calibration period. Based on **Figure 14**, the CDF of simulation flow could capture the shape of the CDF of observed flow with reasonable accuracy on the hourly and daily scale, while on a monthly scale, these two curves are close in low flows and more distant in high flows. **Figure 15** shows that in Timberline location, CDF curves of observed and simulated flows are very tight in all temporal scales. On the monthly scale, there are some parts with overestimation or underestimation, but the overall performance is acceptable.

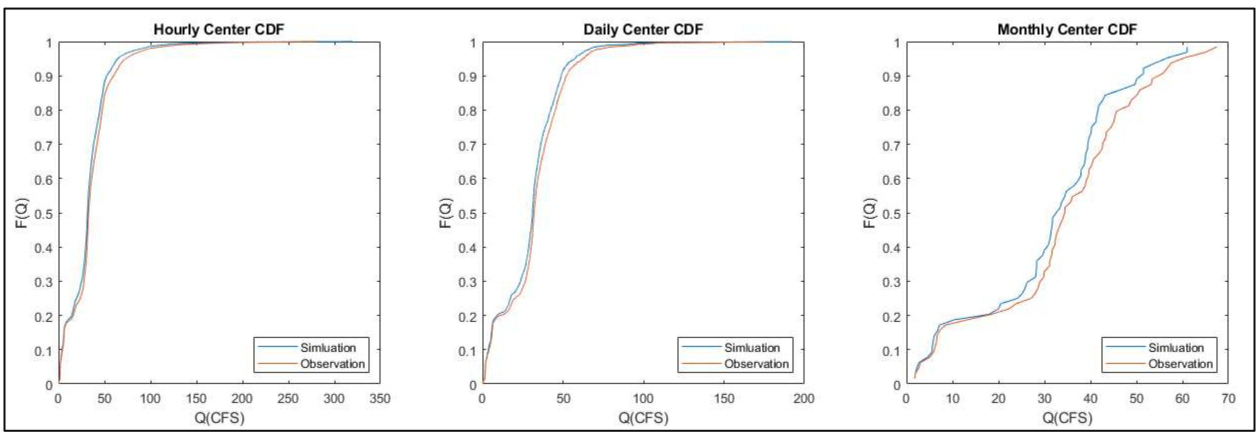

Figure 14: CDF of observed and simulated flow in Center (2008-2014)

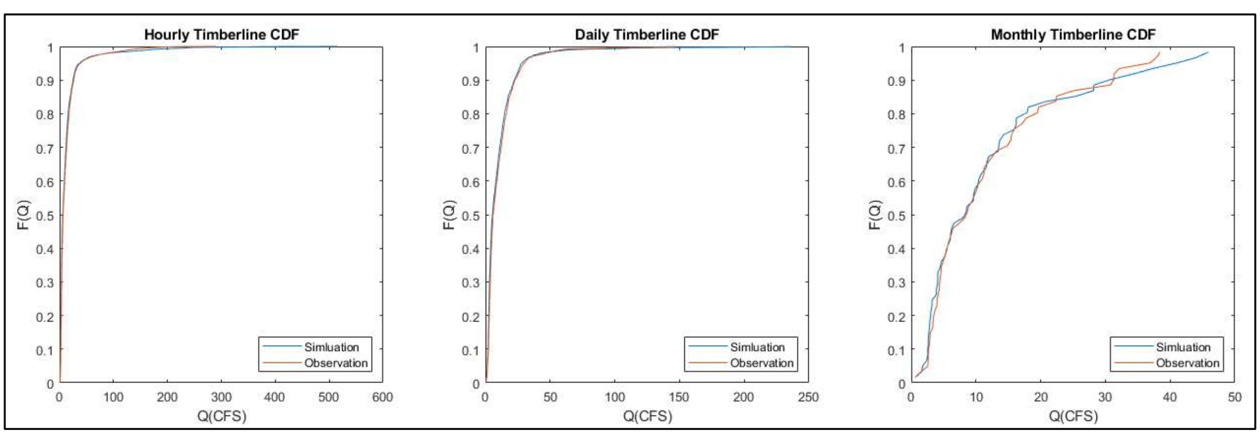

Figure 15: CDF of observed and simulated flow in Timberline (2008-2014)

Flow duration curves of the observed and simulated flows for different temporal scales in both locations are also provided in **Figure 16** and **17**. Both figures indicate that the calibrated model can simulate the exceedance probability of flows with acceptable accuracy.

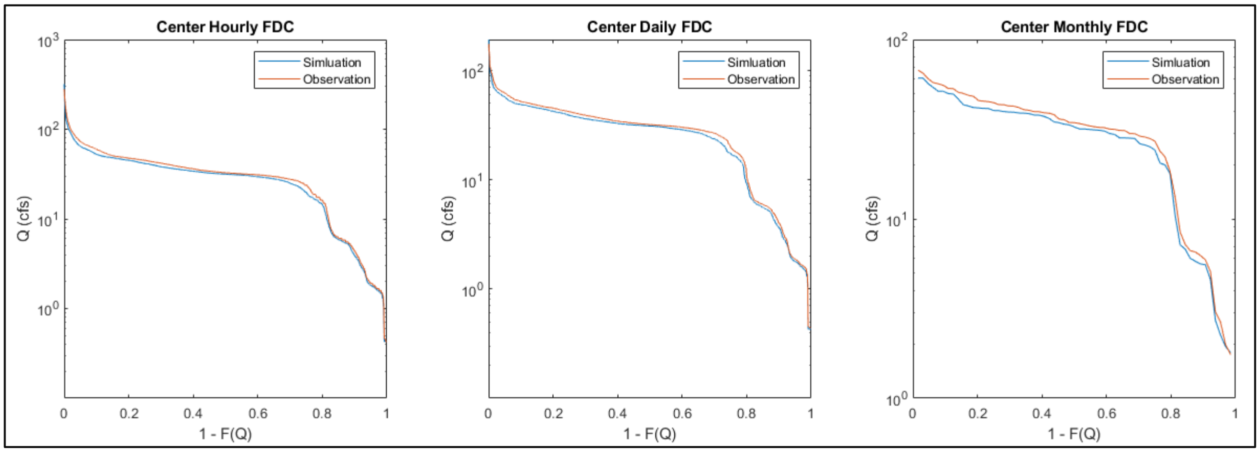

Figure 16: FDC in Center (2008-2014)

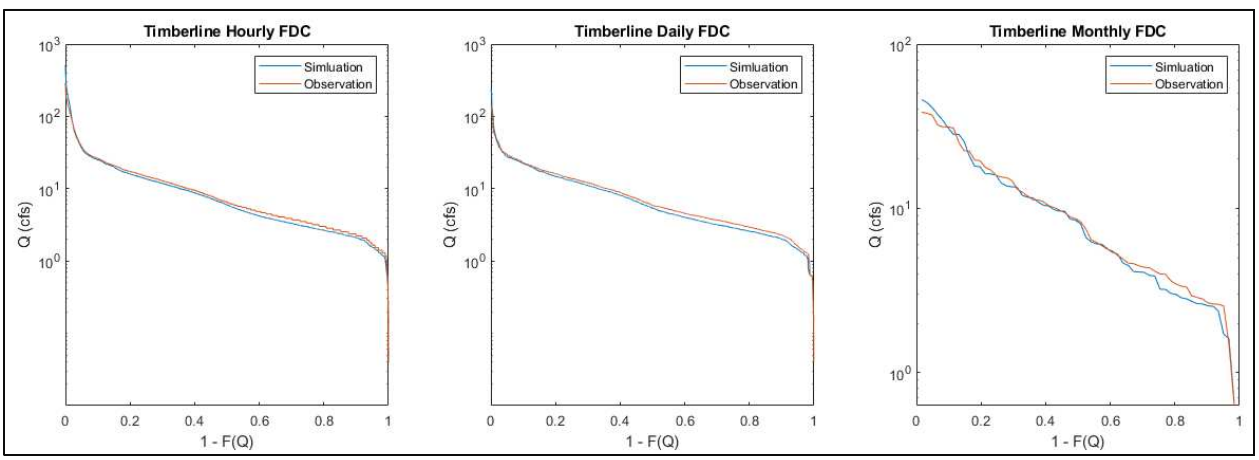

Figure 17: FDC in Timberline (2008-2014)

Figure 18 and **Figure 19** show the time series of observed and simulated flows for different temporal scales in Center and Timberline locations, respectively, for 2015 to 2018. These figures show that the model can predict the shape and peak time of the observed flow very well in both locations. There are some locations in the hourly and daily time series that the model has underestimated or overestimated the peak flows. However, in both locations, the model mostly underestimated the monthly peak flows. Furthermore, as the temporal scale gets bigger, the difference between the observed peak flow and simulated peak flow gets smaller.

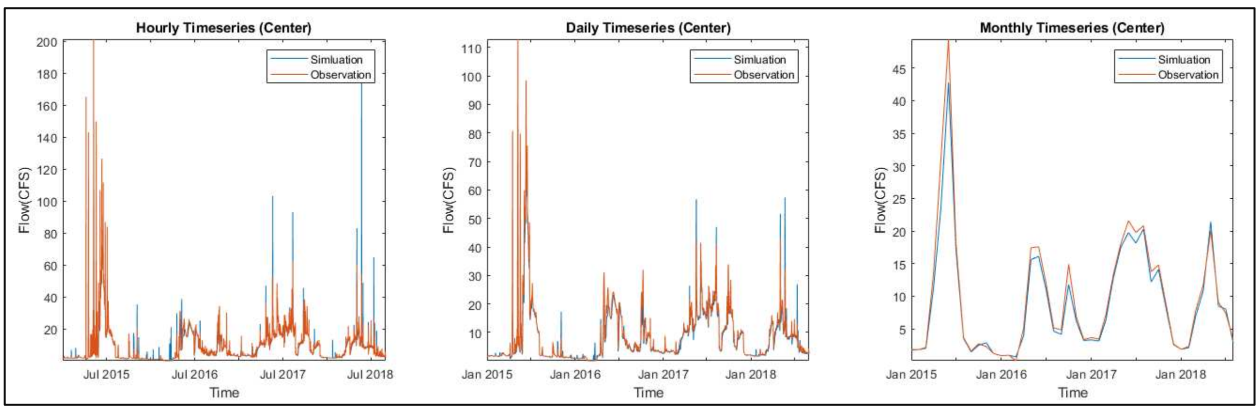

Figure 18: Timeseries of observed and simulated flow in Center (2015-2018)

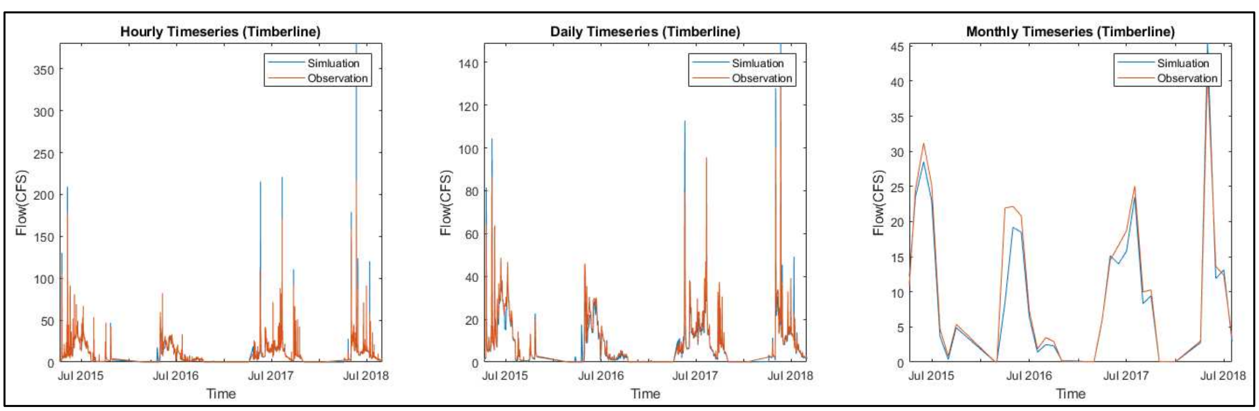

Figure 19: Timeseries of observed and simulated flow in Timberline (2015-2018)

Figure 20 and **Figure 21** show the scatter plots of observed flow versus simulated flow for different temporal scales in Center and Timberline locations, respectively, for 2015 to 2018. These figures show that in the Center location, the model mostly underestimated the flow, and in the Timberline location, flows are mostly underestimated in low to median flows and overestimated in high flows. These plots also show that the points are more scattered with more distance from the 1:1 line in smaller temporal scale, and they get closer to the line as the temporal scale gets larger and show more accuracy in the model prediction.

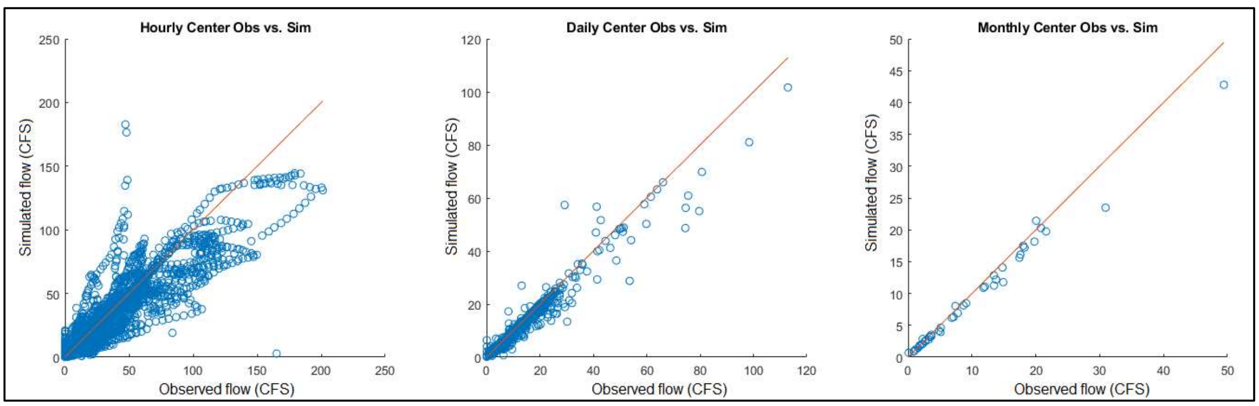

Figure 20: Scatter plots of simulated vs observed flow at Center (2015-2018)

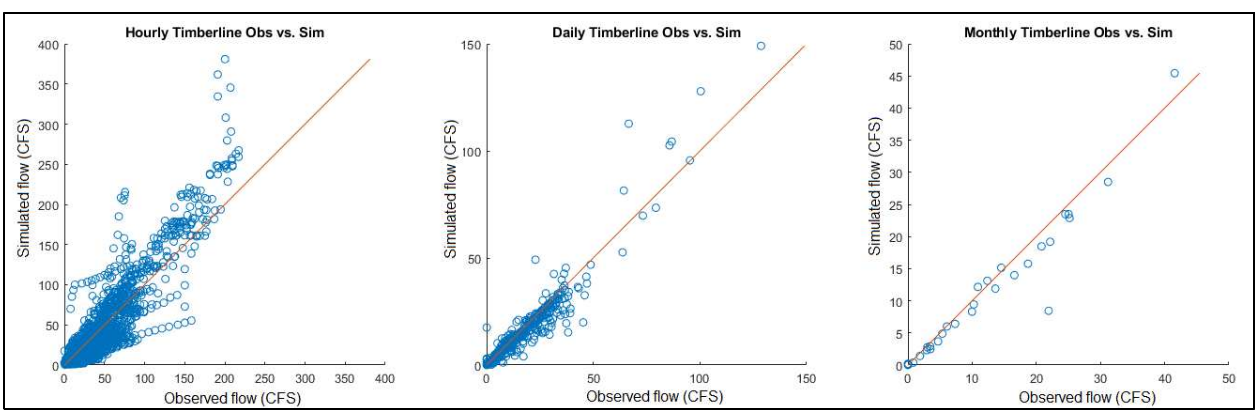

Figure 21: Scatter plots of simulated vs observed flow at Timberline (2015-2018)

Figure 22 and **Figure 23** show the Cumulative Distribution Function (CDF) curves of observed flow and simulated flow for different temporal scales in the Center and Timberline locations, respectively, for 2015 to 2018. Based on **Figure 22**, the CDF of simulation flow can successfully predict the non-exceedance probability of the observed flow. **Figure 23** shows that in Timberline location, CDF curves of observed and simulated flows are very close in all temporal scales. However, on a monthly scale, the model overestimated the non-exceedance probability of the flow above the median, but the overall performance is acceptable.

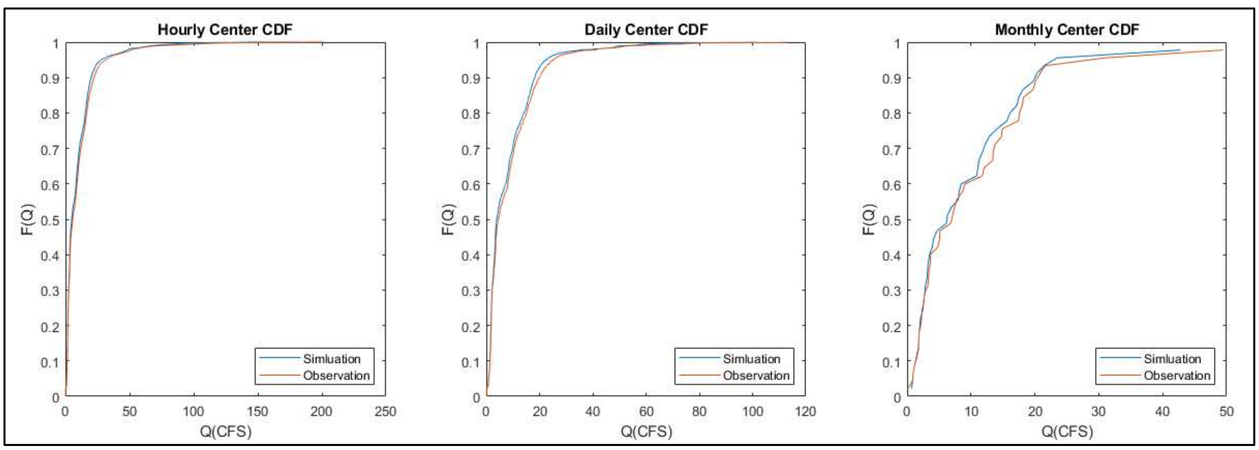

Figure 22: CDF of observed and simulated flow in Center (2015-2018)

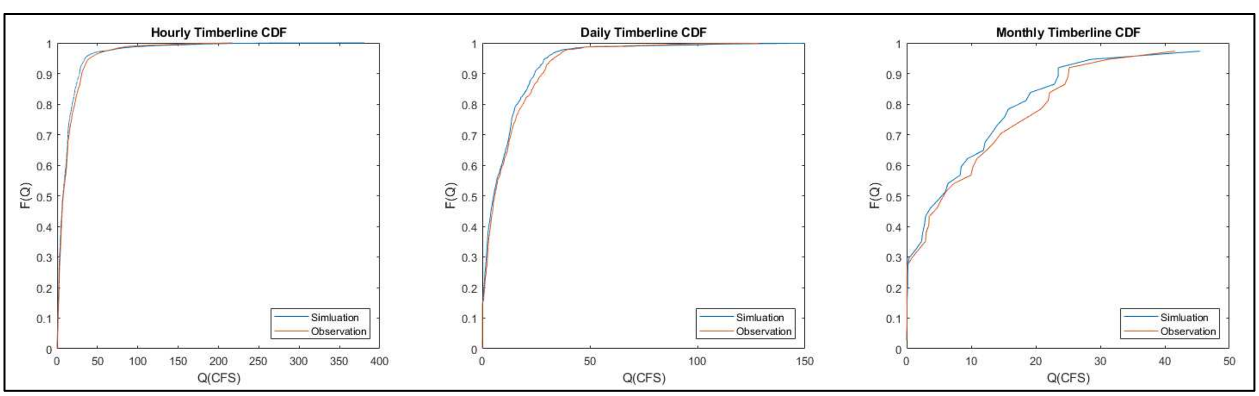

Figure 23: CDF of observed and simulated flow in Timberline (2015-2018)

Flow duration curves of the observed and simulated flows for different temporal scales in both locations are also provided in **Figure 24** and **Figure 25**. Both figures indicate that the calibrated model can simulate the flows with acceptable accuracy. However, in the Timberline location, the model has overestimated the exceedance probability in low flows.

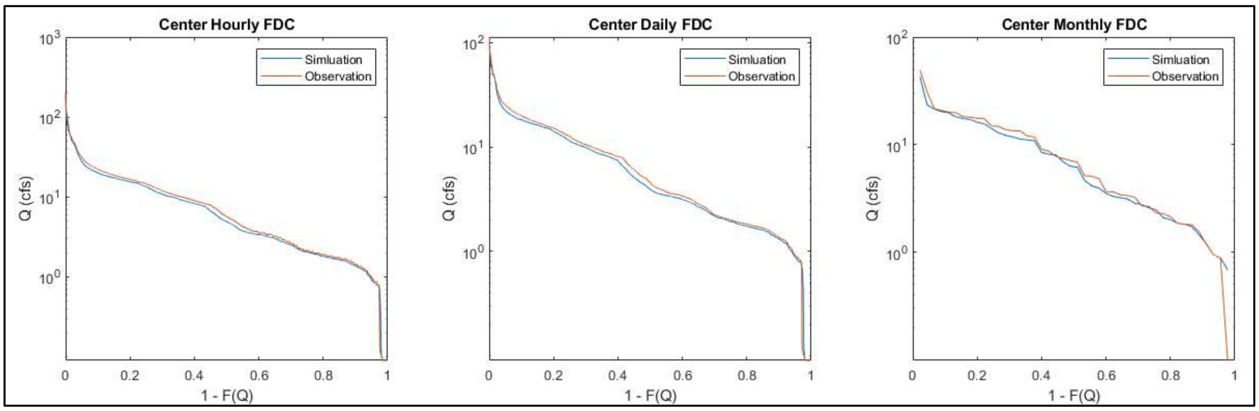

Figure 24: FDC for observed and simulated flow in Center (2015-2018)

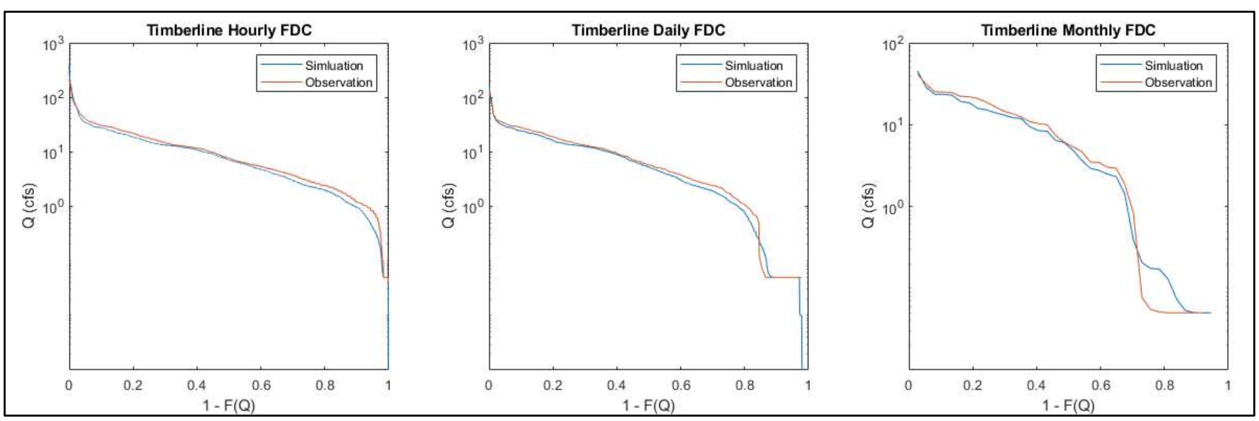

Figure 25: FDC for observed and simulated flow in Timberline (2015-2018)

3.2. CLASIC tool results

After running the CLASIC tool for the desired period, the results of each scenario can be found in the results panel. A SWMM version of each scenario is also available in the results panel that can be downloaded and imported into the SWMM. The first model representing the whole watershed is downloaded, imported into SWMM, and run from 2008 to 2014. Then, the average annual hydrologic components (Runoff, Infiltration, and Evaporation) were extracted from the report file and compared with those from the calibrated SWMM model. **Figure 26** shows the pie charts of both models representing how the total precipitation is divided among hydrologic components. It is understood from this figure that the models report very close fractions for each component. CLASIC has overestimated the runoff compared to the calibrated SWMM model by about 2%, infiltration about 0.5%, and underestimated the evaporation by about 2.5%. It is worth mentioning that the CLASIC tool creates and shows the pie chart of hydrologic components for each scenario in its result panel.

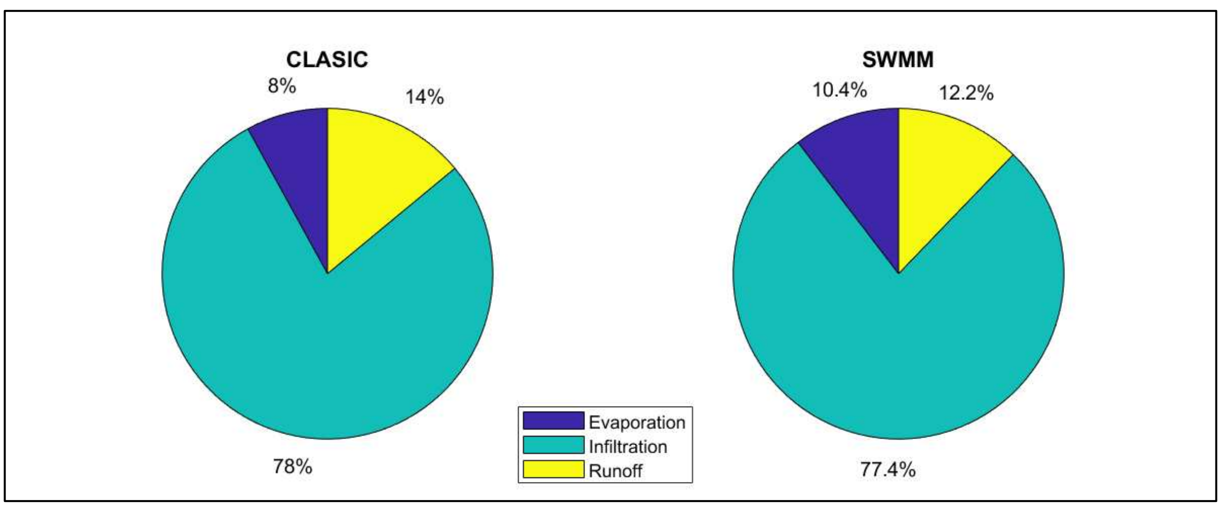

Figure 26: CLASIC vs SWMM in computing the proportion of each hydrologic component in the total precipitation

The second and third CLASIC models were also built in the CLASIC tool and imported into SWMM. Then the total flow at the outlet was then calculated for each model to represent the flow at observation locations. Afterward, the flow for each temporal scale was compared with the observed flows. **Table 5** shows the statistical performance metrics for CLASIC models. It is understood from the Nash-Sutcliff values that the Timberline model is not satisfactory for small temporal scales (hourly and daily), but its performance is good for the monthly scale. In the Center model, the hourly results are not good but still acceptable; however, daily and monthly results are very good. Thus, the CLASIC tool has more accuracy in estimating the flow in the Center location, which is in the middle of the watershed, than in the Timberline location near the outlet. The time of concentration for Center and Timberline locations are about 7 and 10 hours, respectively, and it is understood from Table 5 that although the model does not show good R^2 and NSE on the daily scale, at Timberline location, it has a good PBIAS, and RMSE is not significantly larger than the SD of observed daily flow. Thus, it can be concluded that even in the Timberline location, the CLASIC tool shows an acceptable performance, but not great, for time scales larger than the time of concentration.

Table 5: CLASIC models performance metrics

Location		**PBIAS (%)**	**RMSE (CFS)**	R^2	**NSE**
Center	Hourly	4.7	17.39	0.64	0.54
	Daily	4.95	8.01	0.85	0.83
	Monthly	4.5	3.17	0.97	0.96
Timberline	Hourly	-12.28	38.99	0.36	-2.21
	Daily	-5	17.53	0.50	-0.94
	Monthly	-10.68	4.95	0.88	0.76

Figures 27-34 show the graphical performance measures for CLASIC and SWMM models compared to observed data in Timberline and Center locations. As the time series show, the CLASIC tool has overestimated and underestimated some peaks, but it has captured the peak times and the shape of the observed flow in both locations. Comparison of CLASIC and SWMM indicates that CLASIC has not been successful in attenuating some peak flows, and it has caused extreme peaks at some locations in the time series (e.g., in 2009). Moreover, it is obvious that as the temporal scale gets bigger, the model accuracy gets better.

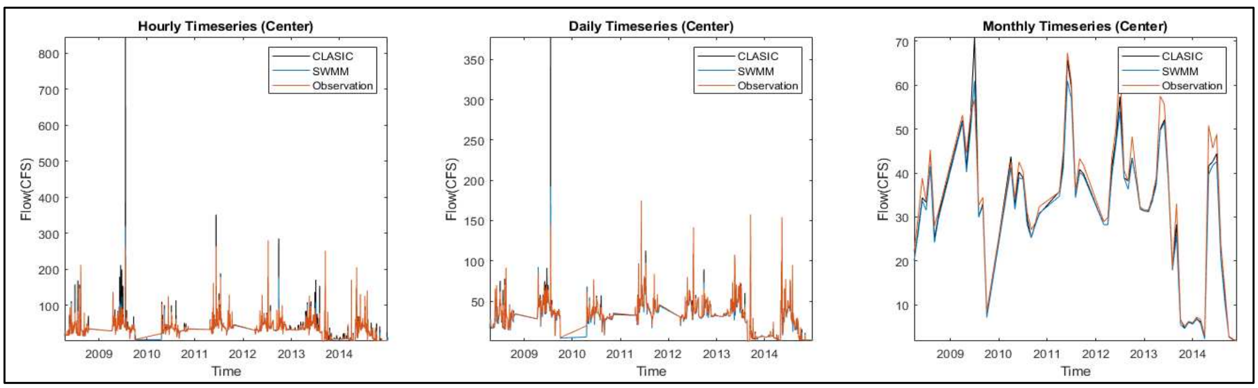

Figure 27: Timeseries of observed and simulated flow (CLASIC and SWMM) in Center

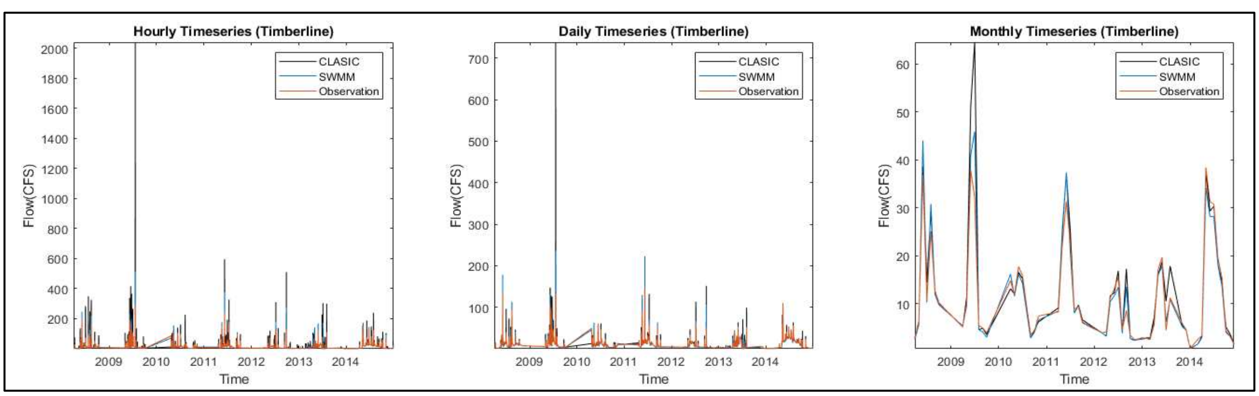

Figure 28: Timeseries of observed and simulated flow (CLASIC and SWMM) in Timberline

Figures 29 and **30** illustrate that SWMM has more accuracy than CLASIC in predicting the observation flow at an hourly time scale. The points are more scattered with CLASIC than SWMM. However, as the time scale gets bigger, CLASIC and SWMM points get closer to each other and to the 1:1 line showing more accuracy in both models.

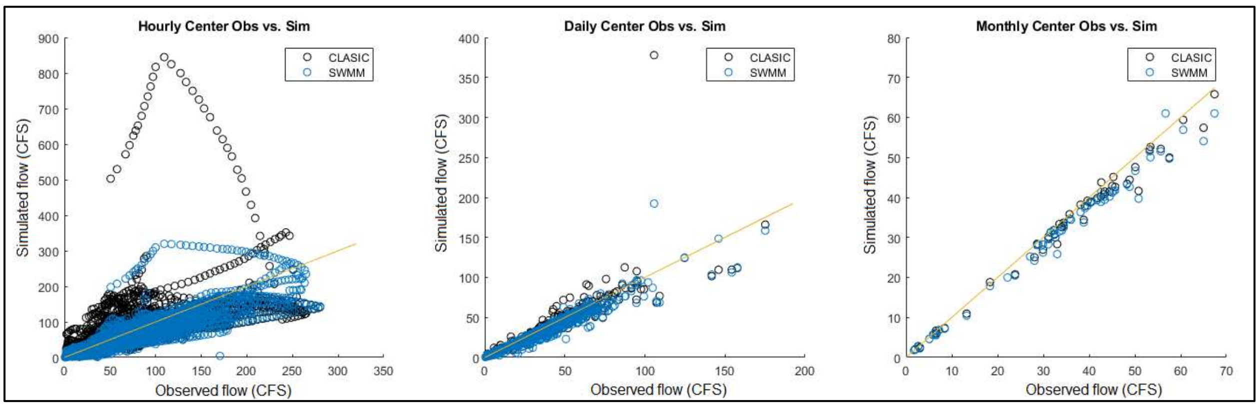

Figure 29: Scatter plots of simulated vs observed flow (CLASIC and SWMM) at Center

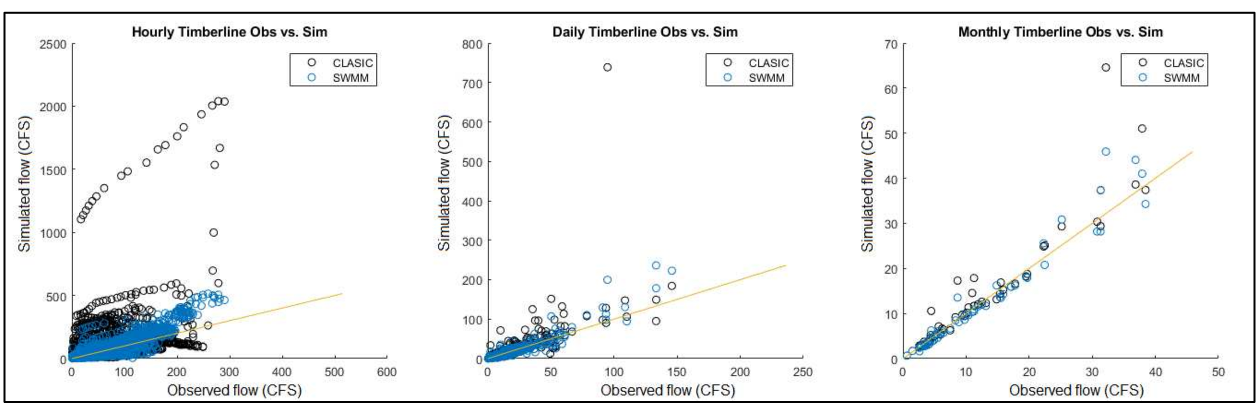

Figure 30: Scatter plots of simulated vs observed flow (CLASIC and SWMM) at Timberline

Moreover, **Figures 31-34** demonstrate that the total flows from CLASIC models have a close probability to the SWMM and observed total flows. In monthly Center CDF curves, it is displayed that SWMM and CLASIC have overestimated the non-exceedance probability of flows. These curves also show that the CLASIC tool CDF is slightly closer to the observation CDF compared to SWMM. However, in the Timberline location, CDF of CLASIC and SWMM have overestimated the observation CDF at some flows and underestimated others. Furthermore, both SWMM and CLASIC CDFs are very close to the observation CDF at this location.

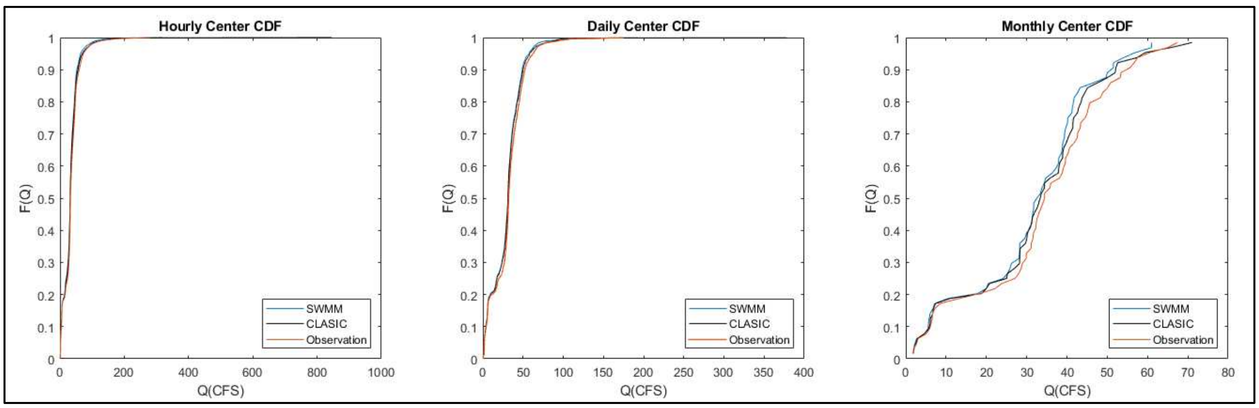

Figure 31: CDF of observed and simulated flow (CLASIC and SWMM) in Center

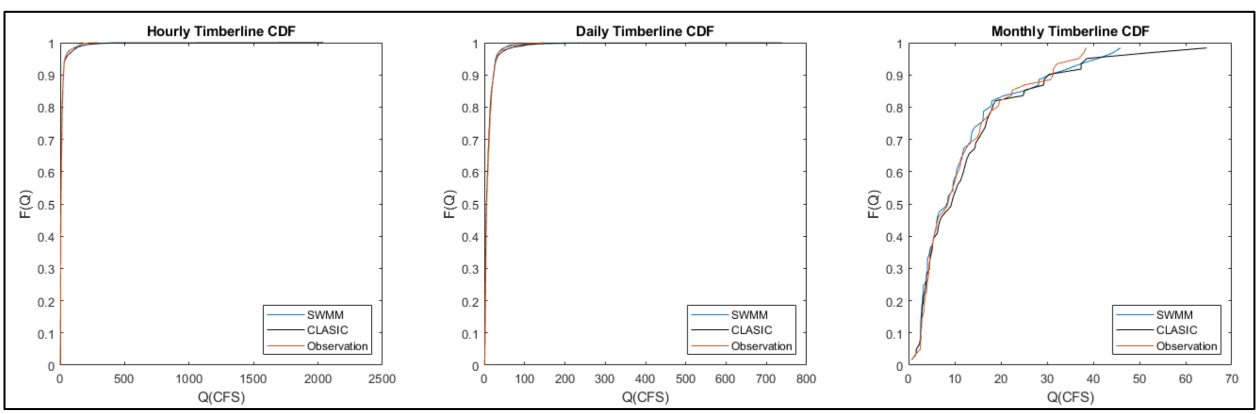

Figure 32: CDF of observed and simulated flow (CLASIC and SWMM) in Timberline

Flow Duration Curves in **Figures 33** and **34** also show that the exceedance probability of the CLASIC and SWMM results are very close to the observed ones. In the Center location monthly plots, however, both models underestimated the percent of the time a given flow is equaled or exceeded. Nevertheless, in the Timberline location monthly plots, the FDC of SWMM and CLASIC have overestimated the observed FDC at some flows and underestimated others.

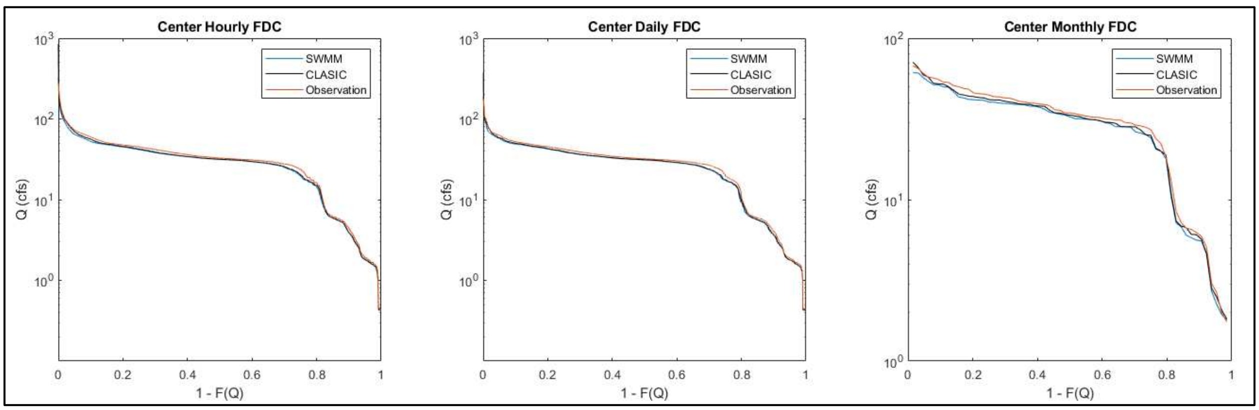

Figure 33: FDC for observed and simulated flow (CLASIC and SWMM) in Center

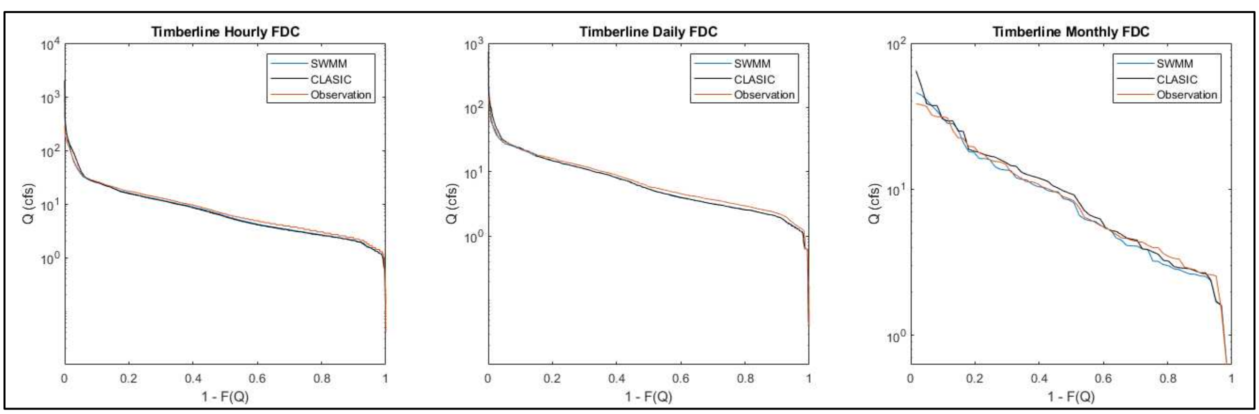

Figure 34:FDC for observed and simulated flow (CLASIC and SWMM) in Timberline

3.3. Sensitivity analysis results

To calculate the sensitivity indices, Average Annual flow, SD of Annual flow, Average Annual Peak flow, and SD of Annual Peak flow from the SWMM model are calculated and imported into SIMLAB for both locations as the target model output for the outputs of all samples. The first order indices (S_i) and total order indices (S_i^T) are presented in **Table 6-9,** and **Figures 35-38**show the Sobol indices pie charts.

The first-order indices should be between zero and one, and the total order indices can be equal or greater than the first-order ones. However, there were some total indices with the value of zero or less than their value of the first order index, and it shows the errors in estimation. Hence, the negative values are replaced with zero in **Tables 6-9**. The sum of the first indices (main effects) can be less than or equal to one, while the sum of total indices can exceed one because some higher-order indices may repeat in some total order indices. **Tables 6-9** also show that the model is non-additive since the sum of the first indices for every target output in both locations is less than one (Nossent et al., 2011).

Table 6: First and Total sensitivity indices for Average Annual flow

Sobol first order indices		
Parameter	*Timberline*	*Center*
Width	0.008	0.008
%Slope	0.013	0.011
%Imperv	0.581	0.578
DstoreImperv	0.054	0.093
DstorePerv	0.002	0.001
%ZeroImperv	0.008	0.004
MaxInfiltration	0.072	0.075
MinInfiltration	0.145	0.138
DecayRate	0.057	0.054
Sum	**0.939**	**0.962**
Sobol total order indices		
Parameter	*Timberline*	*Center*
Width	0.003	0
%Slope	0	0.004
%Imperv	0.586	0.576
DstoreImperv	0.070	0.101
DstorePerv	0.001	0
%ZeroImperv	0.008	0.005
MaxInfiltration	0.149	0.132
MinInfiltration	0.229	0.197
DecayRate	0.108	0.097
Sum	**1.154**	**1.111**
Difference between total and first order indices		
Parameter	*Timberline*	*Center*
Width	0	0
%Slope	0	0
%Imperv	0.005	0
DstoreImperv	0.016	0.009
DstorePerv	0	0
%ZeroImperv	0	0.001
MaxInfiltration	0.076	0.057
MinInfiltration	0.084	0.058
DecayRate	0.051	0.043

Table 7: First and Total sensitivity indices for Average Annual peak flow

Sobol first order indices		
Parameter	*Timberline*	*Center*
Width	0.012	0.011
%Slope	0.016	0.018
%Imperv	0.418	0.146
DstoreImperv	0.025	0.002
DstorePerv	0.011	0.018
%ZeroImperv	0.022	0.005
MaxInfiltration	0.115	0.237
MinInfiltration	0.136	0.224
DecayRate	0.076	0.171
Sum	**0.831**	**0.832**
Sobol total order indices		
Parameter	*Timberline*	*Center*
Width	0.043	0.016
%Slope	0.027	0.011
%Imperv	0.470	0.143
DstoreImperv	0.084	0.014
DstorePerv	0.027	0.029
%ZeroImperv	0.056	0.017
MaxInfiltration	0.227	0.338
MinInfiltration	0.266	0.340
DecayRate	0.203	0.249
Sum	**1.403**	**1.157**
Difference between total and first order indices		
Parameter	*Timberline*	*Center*
Width	0.031	0.004
%Slope	0.011	0
%Imperv	0.052	0
DstoreImperv	0.059	0.012
DstorePerv	0.016	0.011
%ZeroImperv	0.034	0.013
MaxInfiltration	0.112	0.101
MinInfiltration	0.130	0.116
DecayRate	0.127	0.079

Table 8: First and Total sensitivity indices for SD of Annual flow

Sobol first order indices		
Parameter	*Timberline*	*Center*
Width	0.009	0.013
%Slope	0.010	0.008
%Imperv	0.325	0.230
DstoreImperv	0.009	0.007
DstorePerv	0.011	0.009
%ZeroImperv	0.012	0.005
MaxInfiltration	0.201	0.251
MinInfiltration	0.131	0.149
DecayRate	0.132	0.158
Sum	**0.839**	**0.830**
Sobol total order indices		
Parameter	*Timberline*	*Center*
Width	0.015	0
%Slope	0.010	0.012
%Imperv	0.352	0.239
DstoreImperv	0.049	0.014
DstorePerv	0.016	0.013
%ZeroImperv	0.030	0.005
MaxInfiltration	0.281	0.316
MinInfiltration	0.232	0.239
DecayRate	0.220	0.221
Sum	**1.205**	**1.059**
Difference between total and first order indices		
Parameter	*Timberline*	*Center*
Width	0.007	0
%Slope	0.000	0.004
%Imperv	0.028	0.009
DstoreImperv	0.040	0.007
DstorePerv	0.005	0.004
%ZeroImperv	0.019	0.000
MaxInfiltration	0.080	0.064
MinInfiltration	0.101	0.090
DecayRate	0.088	0.063

Table 9: First and Total sensitivity indices for SD of Annual peak flow

Sobol first order indices		
Parameter	*Timberline*	*Center*
Width	0	0.013
%Slope	0	0.022
%Imperv	0.219	0.050
DstoreImperv	0.049	0.001
DstorePerv	0.010	0.019
%ZeroImperv	0.032	0.004
MaxInfiltration	0.183	0.410
MinInfiltration	0.019	0.089
DecayRate	0.070	0.232
Sum	**0.582**	**0.841**
Sobol total order indices		
Parameter	*Timberline*	*Center*
Width	0.159	0.019
%Slope	0.145	0.041
%Imperv	0.398	0.054
DstoreImperv	0.245	0.009
DstorePerv	0.134	0.031
%ZeroImperv	0.220	0.011
MaxInfiltration	0.333	0.452
MinInfiltration	0.208	0.141
DecayRate	0.318	0.271
Sum	**2.161**	**1.029**
Difference between total and first order indices		
Parameter	*Timberline*	*Center*
Width	0.159	0.006
%Slope	0.145	0.018
%Imperv	0.178	0.004
DstoreImperv	0.196	0.008
DstorePerv	0.124	0.012
%ZeroImperv	0.188	0.007
MaxInfiltration	0.150	0.042
MinInfiltration	0.190	0.052
DecayRate	0.249	0.039

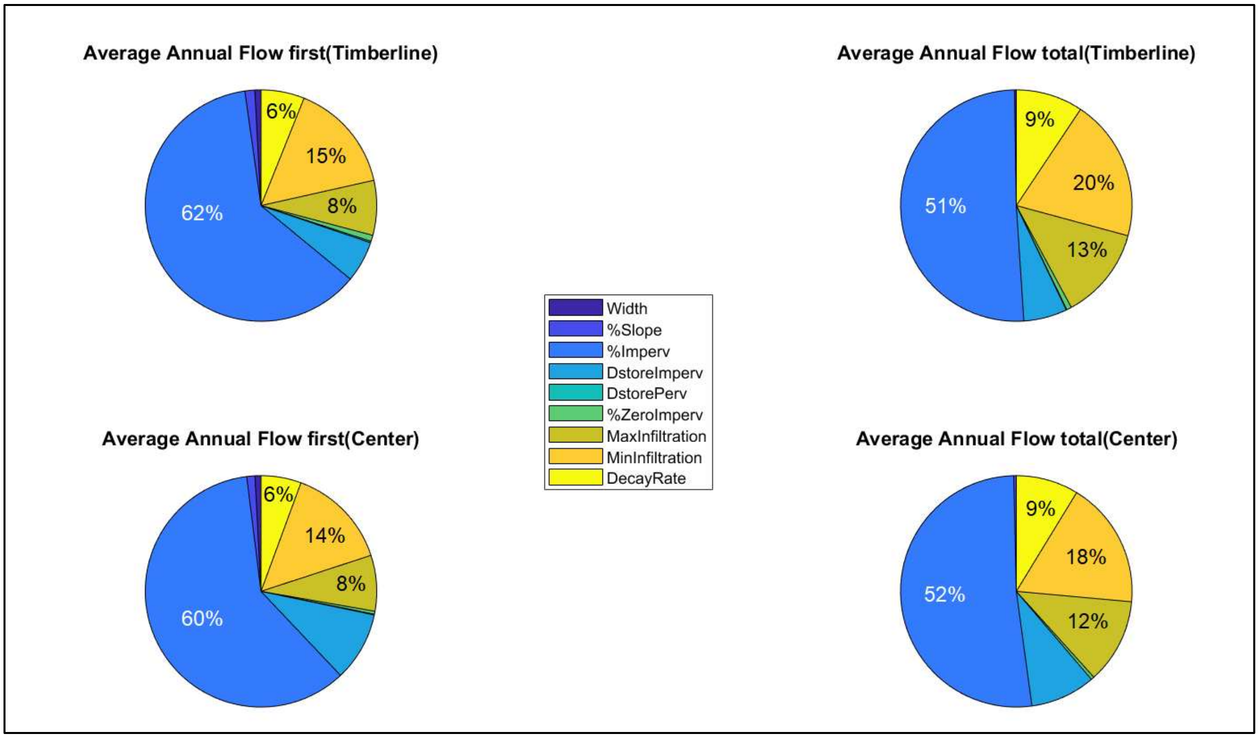

Figure 35: Average Annual flow indices

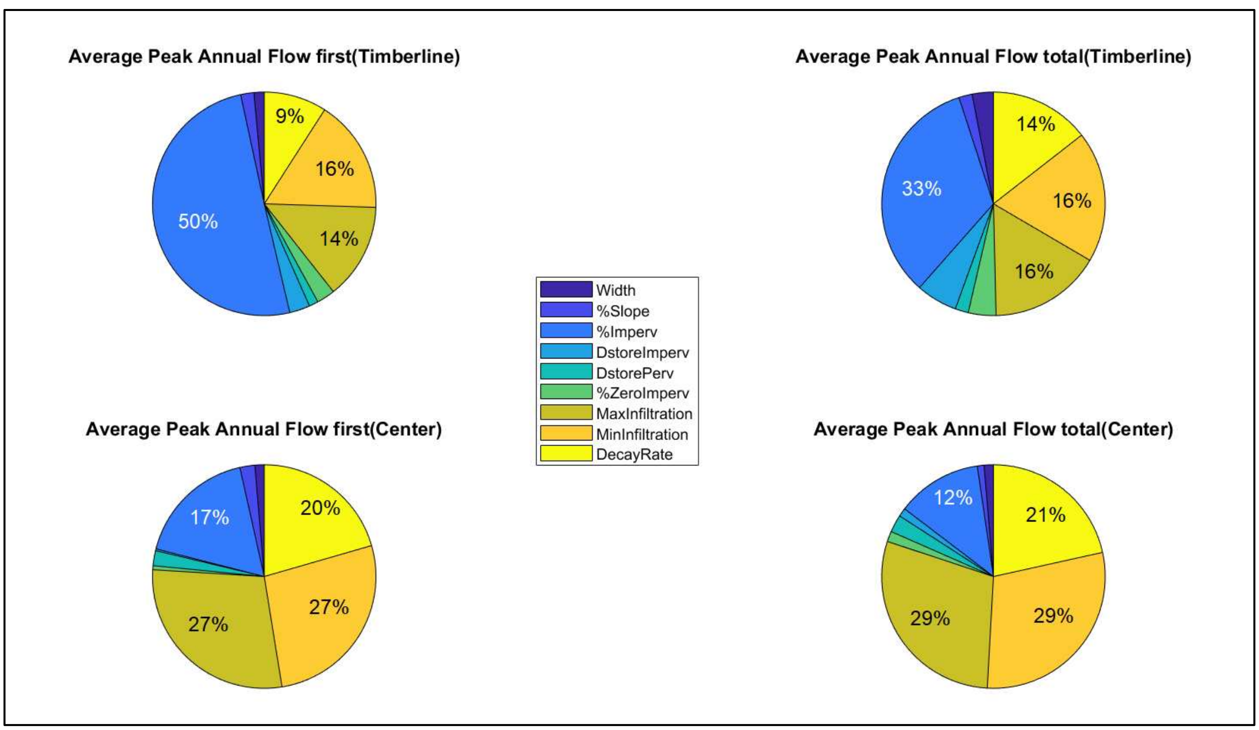

Figure 36: Average Annual Peak flow indices

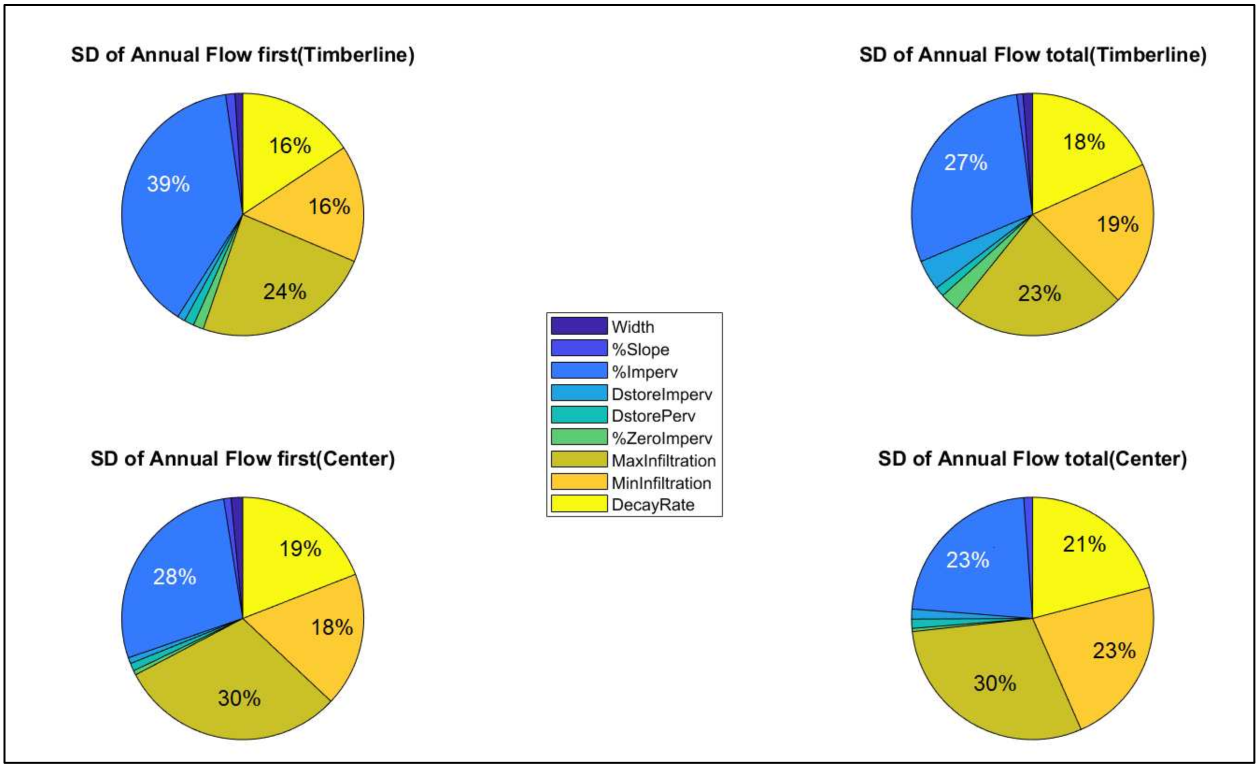

Figure 37: Standard Deviation of Annual flow indices

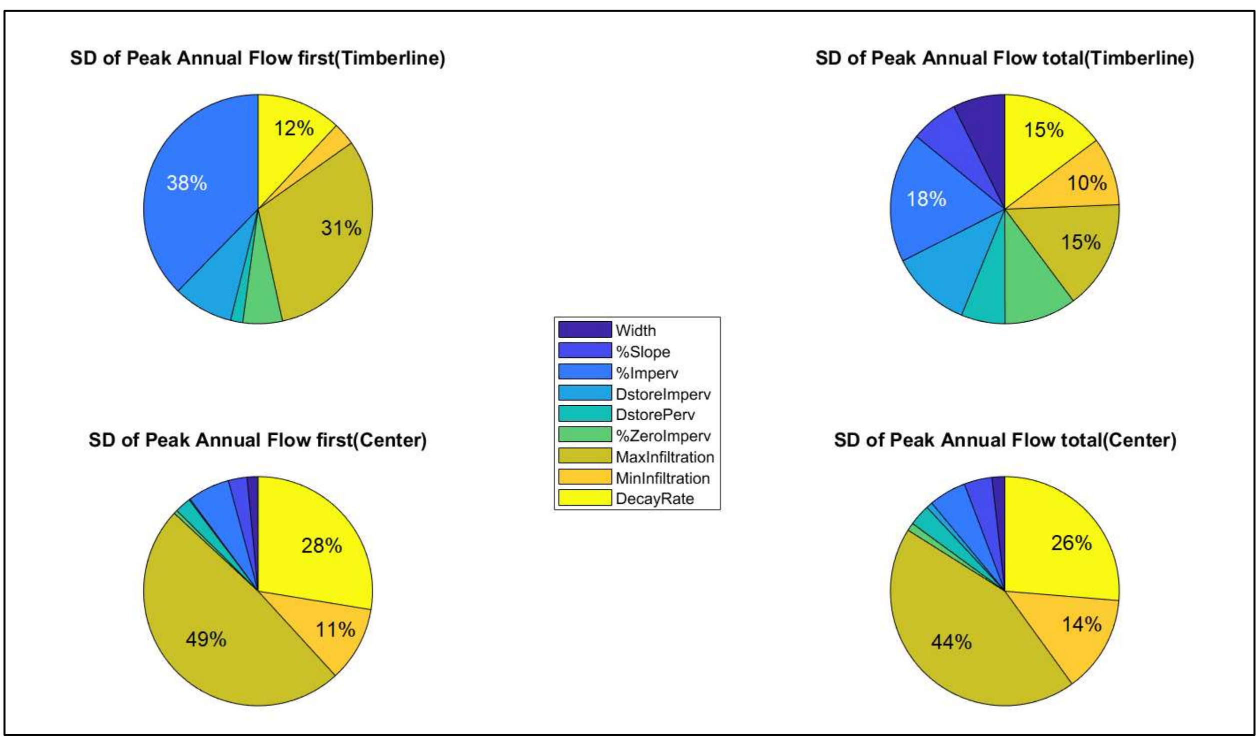

Figure 38: Standard Deviation of Annual Peak flow indices

Table 6 and **Figure 35** show the sensitivity indices for the average annual flow as a target output of the model. Based on the first order and total order indices, the most important factor for the average annual flow of the Spring Creek in both locations is the percent of imperviousness (%Imperv). Thus, the variance of the average annual flow is most sensitive to this factor, and by fixing this factor to its actual value, there would be a significant reduction in the output variance. The difference between the total index and first-order index of this output is not very substantial, meaning that this input factor has a low interaction with other factors. The most important factors after %Imperv, for the Timberline location, are Minimum infiltration rate, Maximum infiltration rate, Decay rate, and Depression storage of impervious area, based on the order of their importance. The difference between their first and total order indices indicates that they have the same order of importance in their interactions with other factors. The rest of the factors are not very important because they have very small S_i and S_i^T.

The most important factors after %Imperv, for the Center location, are Minimum infiltration rate, Depression storage of impervious area, Maximum infiltration rate, and Decay rate, and Minimum infiltration rate has the most interaction with other parameters in the total variance of the output.

With the same approach, **Table 7** and **Figure 36** show that in Timberline location, the most important factor, in terms of the individual effect on the average annual peak flow, is the percent of imperviousness, and by fixing this factor to its actual value, there would be a great reduction in the variance of the output. After this factor, Minimum infiltration rate, Maximum infiltration rate, and Decay rate are important. However, in terms of interactions, the Minimum infiltration rate has the most significant difference between its first order and total order; hence, this factor has the most interaction with other factors among all the factors followed by Decay rate, Max infiltration rate, Depression storage of impervious area, and %ZeroImperv. Other factors are not as important as the mentioned ones.

In the Center location, however, the percent of imperviousness is the 4th important factor among all factors, in terms of the main effect. Maximum infiltration rate followed by Minimum infiltration rate and the Decay rate are the most important factors. In terms of interaction, the factors have the same ranks. Other factors are not very important.

From **Table 8** and **Figure 37**, it is concluded that for Timberline location, the most important factor for SD of annual flow is the percent of imperviousness because it has the biggest S_i and S_i^T. After this factor, Maximum infiltration rate, Decay rate, and Minimum infiltration rate are the most important factors. In terms of interaction with other factors, however, the Minimum infiltration rate has the greatest effect, followed by Decay rate and Maximum infiltration rate. Other factors are not very important.

Center location shows a different order of importance. The difference is that in this location, the Maximum infiltration rate is more important than the percent of imperviousness. The factors with most interactions with others are also the same as Timberline, while Maximum infiltration rate has more interaction than Decay rate.

Table 9 and **Figure 38** indicate that the important factors for the SD of peak annual flows are very different in the two locations. The percent of imperviousness is the most important factor in Timberline, while it is ranked 4 in Center, and Maximum infiltration rate is the most important one in this location. Nevertheless, Maximum infiltration rate is the second important factor in Timberline, while its S_i is close to the first important factor. Moreover, Width and %Slope have zero S_i in Timberline, while they have a small value of S_i in Center. Decay rate has the 3rd rank in Timberline and second rank in Center, in terms of the main effect. Depression storage of impervious area has the 4th rank in Timberline location, while it is the least important factor in Center location. An interesting conclusion for Timberline, based on the table, is that all other factors with very small S_i have significant and almost close S_i^T's. This means that although these factors do not have strong individual effect on the output, they have big interactions in higher orders.

4. Discussion

Comparing the results of the CLASIC tool and SWMM model with the observed data indicated that SWMM has a better estimation of total flow at smaller computational time scales than the CLASIC tool. It results from removing the conveyance system and using dummy conduits that do not account for attenuating flow since the CLASIC tool is not intended to be used for flood control (Dell et al., 2021). It is understood from the results that the time of concentration may have an essential role in the performance of the CLASIC tool. The model performance at the Center location was very good at the daily and monthly time scales, but at the Timberline location, only the monthly results are very good. Although the time of concentration is less than a day at the Timberline location and PBIAS and RMSE are reasonable at the daily time scale, NSE is not acceptable. The time series and scatterplots can explain the reason. The significant peak flow in July 2009 had more effect on the Timberline results than Center results. The size of the peak flow in the CLASIC tool is about five times the size of the observed peak flow at that time in the Timberline location, while it is about three times in the Center location. It may be due to the size of the upstream drainage area of each gauged location, which was bigger for Timberline than Center. The effect of the big storm in 2009 is also apparent when we compare the performance of the calibrated SWMM model of 2008-2014 with 2015-2018. The model performed better in 2015-2018 than the calibration period since there was no such storm in that period.

Another important point to consider is that in the CLASIC results, the model parameters are based on the calibrated SWMM model; hence they may not be the optimal value for the CLASIC model.

By looking at the flow duration curves, it is understood that although the flow simulated by the CLASIC tool and SWMM model had some discrepancies with the observed flow, especially in smaller time scales, both models had a great estimate of flow statistics.

5. Conclusion

Population growth and rapid urbanization have led municipalities to look for more sustainable alternatives for their current stormwater infrastructures. CLASIC tool is an easy-to-use web tool developed to help decision-makers better plan for their future stormwater infrastructures by comparing different scenarios in terms of reduction in runoff and pollutant loads, costs, and co-benefits. This study evaluated and compared the hydrologic responses of the CLASIC tool to a complex SWMM model to inform the decision-makers about the performance validity of this tool which requires fewer parameters and effort than a complex model to simulate the hydrologic responses,

The results of the models showed that the CLASIC tool performs well in estimating the hydrologic components (the portion of precipitation allocated to runoff, infiltration, and evaporation) compared to the calibrated full SWMM model, and the models report very close values for each component. Thus, it is concluded that the CLASIC tool can help the modeler assess the water balance in a watershed easier and with fewer parameters.

Moreover, the Center and Timberline models showed that the CLASIC tool can estimate the total flow for monthly scale with good accuracy in both locations. However, the analysis showed a significant peak in the time series of flows in July 2009 caused by a big storm. Furthermore, Nash-Sutcliff overestimates the big errors and underestimates the small ones since all the errors are squared (Krause et al., 2005). Thus, SWMM has a better performance in estimating this peak flow than the CLASIC tool since CLASIC uses a simpler routing method that does not account for flow attenuation, and as a result, the NSE values for SWMM is better than the CLASIC tool. Hence, although the CLASIC tool is not developed for flow analysis, it performed acceptably in the Spring Creek for temporal scales greater than the time of concentration.

It is understood from the sensitivity analysis results that the order of importance of the parameters is different for different target outputs and locations; however, the overall conclusion is that the parameters of the Horton infiltration method and the percent of imperviousness are the most important factors in the Spring Creek watershed, and "depression storage in the impervious area" is important in some cases.

To better judge the performance of the CLASIC tool in assessing the hydrologic components, it is recommended to test the tool in other watersheds inside and outside of Colorado, with different scales and for different types of LID control systems. Moreover, other modules of the CLASIC tool were not discussed in this project, so future studies can be focused on working with other modules of the tool as well as developing the system identification and optimization components that enable the selection of systems that are most consistent with the desired goals of planners, including hydrologic effects, co-benefits, and life cycle costs.

6. References

Andraddttir, S., Healy, K. J., Withers, D. H., & Nelson, B. L. (1997). S. Andraddttir, K. *Simulation*, 261–268.

Archer, G. E. B., Saltelli, A., & Sobol, I. M. (1997). Sensitivity measures, anova-like techniques and the use of bootstrap. *Journal of Statistical Computation and Simulation*, *58*(2), 99–120. https://doi.org/10.1080/00949659708811825

Babaei, S., Ghazavi, R., & Erfanian, M. (2018). Urban flood simulation and prioritization of critical urban sub-catchments using SWMM model and PROMETHEE II approach. *Physics and Chemistry of the Earth*, *105*(February), 3–11. https://doi.org/10.1016/j.pce.2018.02.002

Baroni, G., & Francke, T. (2020). An effective strategy for combining variance- and distribution-based global sensitivity analysis. *Environmental Modelling and Software*, *134*(September), 104851. https://doi.org/10.1016/j.envsoft.2020.104851

Becker, D. (2014). *Overview of advantages and drawbacks of different methods for sensitivity analysis in the context of performance assessment*. *October*.

Beven, K. (2001). How far can we go in distributed hydrological modelling? *Hydrology and Earth System Sciences*, *5*(1), 1–12. https://doi.org/10.5194/hess-5-1-2001

Brown, A. E., Zhang, L., McMahon, T. A., Western, A. W., & Vertessy, R. A. (2005). A review of paired catchment studies for determining changes in water yield resulting from alterations in vegetation. *Journal of Hydrology*, *310*(1–4), 28–61. https://doi.org/10.1016/j.jhydrol.2004.12.010

Burgan, H. I., & Aksoy, H. (2018). Annual flow duration curve model for ungauged basins.

Hydrology Research, *49*(5), 1684–1695. https://doi.org/10.2166/nh.2018.109

Burgan, H. I., & Aksoy, H. (2020). Monthly flow duration curve model for ungauged river basins. *Water (Switzerland)*, *12*(2), 1–19. https://doi.org/10.3390/w12020338

Campolongo, F., Cariboni, J., & Saltelli, A. (2007). An effective screening design for sensitivity analysis of large models. *Environmental Modelling and Software*, *22*(10), 1509–1518. https://doi.org/10.1016/j.envsoft.2006.10.004

Catena Analytics. (2020). User Guide User Guide. *Computer*, *0*(September), 169–232. www.impact-test.co.uk

Cibin, R., Athira, P., Sudheer, K. P., & Chaubey, I. (2014). *Application of distributed hydrological models for predictions in ungauged basins : a method to quantify predictive uncertainty*. *2045*(March 2013), 2033–2045. https://doi.org/10.1002/hyp.9721

Cipolla, S. S., Maglionico, M., & Stojkov, I. (2016). A long-term hydrological modelling of an extensive green roof by means of SWMM. *Ecological Engineering*, *95*, 876–887. https://doi.org/10.1016/j.ecoleng.2016.07.009

Dell, T., Razzaghmanesh, M., Sharvelle, S., & Arabi, M. (2021). Development and Application of a SWMM-Based Simulation Model for Municipal Scale Hydrologic Assessments. *Water*, *13*(12), 1644. https://doi.org/10.3390/w13121644

DiLoreto, G., Hara, M., Kmiec, J., Neumann, K., Olson, D., Peterson, C., Pierce, L., Schlaman, J., Shah, A., & Szafran, J. (2020). *The Economic Benefits of Investing in Water Infrastructure: How a Failure to Act Would Affect the US Ecnomic Recovery*.

Giap, G. E., & Kosuke, N. (2014). *Sensitivity Analysis Using Sobol ‘ Variance-Based Method on* *the Haverkamp Constitutive Functions Implemented in Richards ' Water Flow Equation*. *18*, 19–33.

Hammit, S. . (2010). *Toward Sustainable Stormwater Management: Overcoming Barriers to Green Infrastructure*. 1–103. https://dspace.mit.edu/handle/1721.1/59735

Hamouz, V., & Muthanna, T. M. (2019). Hydrological modelling of green and grey roofs in cold climate with the SWMM model. *Journal of Environmental Management*, *249*(July), 109350. https://doi.org/10.1016/j.jenvman.2019.109350

Haris, H., Chow, M. F., Usman, F., Sidek, L. M., Roseli, Z. A., & Norlida, M. D. (2016). Urban Stormwater Management Model and Tools for Designing Stormwater Management of Green Infrastructure Practices. *IOP Conference Series: Earth and Environmental Science*, *32*(1). https://doi.org/10.1088/1755-1315/32/1/012022

Horton, R. E. (1941). An Approach Toward a Physical Interpretation of Infiltration-Capacity. *Soil Science Society of America*. https://doi.org/10.2136/sssaj1941.036159950005000C0075x

James, W., & Rossman, L. A. (2003). *User ' S Guide To Swmm5*.

Jang, S., Cho, M., Yoon, J., Yoon, Y., Kim, S., Kim, G., Kim, L., & Aksoy, H. (2007). Using SWMM as a tool for hydrologic impact assessment. *Desalination*, *212*(1–3), 344–356. https://doi.org/10.1016/j.desal.2007.05.005

Jayasooriya, V. M., & Ng, A. W. M. (2014). Tools for modeling of stormwater management and economics of green infrastructure practices: A review. *Water, Air, and Soil Pollution*, *225*(8). https://doi.org/10.1007/s11270-014-2055-1

Khorashadi, F., Nossent, J., Sarrazin, F., Pianosi, F., Griensven, A. Van, Wagener, T., & Bauwens, W. (2017). Environmental Modelling & Software Comparison of variance-based and moment-independent global sensitivity analysis approaches by application to the SWAT model. *Environmental Modelling and Software*, *91*, 210–222. https://doi.org/10.1016/j.envsoft.2017.02.001

Kong, F., Ban, Y., Yin, H., James, P., & Dronova, I. (2017). Modeling stormwater management at the city district level in response to changes in land use and low impact development. *Environmental Modelling and Software*, *95*, 132–142. https://doi.org/10.1016/j.envsoft.2017.06.021

Koo, H., Chen, M., Jakeman, A. J., & Zhang, F. (2020). A global sensitivity analysis approach for identifying critical sources of uncertainty in non-identifiable , spatially distributed environmental models : A holistic analysis applied to SWAT for input datasets and model parameters. *Environmental Modelling and Software*, *127*(February), 104676. https://doi.org/10.1016/j.envsoft.2020.104676

Krause, P., Boyle, D. P., & Bäse, F. (2005). Comparison of different efficiency criteria for hydrological model assessment. *Advances in Geosciences*, *5*, 89–97. https://doi.org/10.5194/adgeo-5-89-2005

Leimgruber, J., Krebs, G., Camhy, D., & Muschalla, D. (2018). *Sensitivity of Model-Based Water Balance to Low Impact Development Parameters*. https://doi.org/10.3390/w10121838

Leong, C., & Yokoo, Y. (2021). A step toward global-scale applicability and transferability of flow duration curve studies: A flow duration curve review (2000–2020). *Journal of*

Hydrology, *603*(PB), 126984. https://doi.org/10.1016/j.jhydrol.2021.126984

Li, C., Liu, M., Hu, Y., Shi, T., Zong, M., & Walter, M. T. (2018). Assessing the impact of urbanization on direct runoff using improved composite CN method in a large urban area. *International Journal of Environmental Research and Public Health*, *15*(4). https://doi.org/10.3390/ijerph15040775

Li, J., Duan, Q., & Gong, W. (2013). *Assessing parameter importance of the Common Land Model based on Assessing parameter importance of the Common Land Model based on qualitative and quantitative sensitivity analysis*. *June 2016*. https://doi.org/10.5194/hess-17-3279-2013

Lim, K. J., Engel, B. A., Tang, Z., & Choi, J. (2006). *AUTOMATED WEB GIS BASED HYDROGRAPH ANALYSIS TOOL , WHAT 1*. *1397*, 1407–1416.

Loague, K., & Green, R. E. (1991). Statistical and graphical methods for evaluating solute transport models: Overview and application. *Journal of Contaminant Hydrology*, *7*(1–2), 51–73. https://doi.org/10.1016/0169-7722(91)90038-3

Locatelli, L., Mark, O., Mikkelsen, P. S., Arnbjerg-Nielsen, K., Deletic, A., Roldin, M., & Binning, P. J. (2017). Hydrologic impact of urbanization with extensive stormwater infiltration. *Journal of Hydrology*, *544*, 524–537. https://doi.org/10.1016/j.jhydrol.2016.11.030

MacMullan, E., & Reich, S. (2007). *The Economics of Low-Impact Development: A Literature Review*. *November*, 1–40. papers2://publication/uuid/52B0BE84-AD08-4E0A-BCA5-F96AFB6133E8

McGrane, S. J. (2016). Impacts of urbanisation on hydrological and water quality dynamics, and urban water management: a review. *Hydrological Sciences Journal*, *61*(13), 2295–2311. https://doi.org/10.1080/02626667.2015.1128084

Miller, J. D., Kim, H., Kjeldsen, T. R., Packman, J., Grebby, S., & Dearden, R. (2014). Assessing the impact of urbanization on storm runoff in a peri-urban catchment using historical change in impervious cover. *Journal of Hydrology*, *515*, 59–70. https://doi.org/10.1016/j.jhydrol.2014.04.011

Moriasi, D. N., Gitau, M. W., Pai, N., & Daggupati, P. (2015). Hydrologic and water quality models: Performance measures and evaluation criteria. *Transactions of the ASABE*, *58*(6), 1763–1785. https://doi.org/10.13031/trans.58.10715

Müller, M. F., & Thompson, S. E. (2016). Comparing statistical and process-based flow duration curve models in ungauged basins and changing rain regimes. *Hydrology and Earth System Sciences*, *20*(2), 669–683. https://doi.org/10.5194/hess-20-669-2016

Nguyen, A. T., & Reiter, S. (2015). A performance comparison of sensitivity analysis methods for building energy models. *Building Simulation*, *8*(6), 651–664. https://doi.org/10.1007/s12273-015-0245-4

Nossent, J., Elsen, P., & Bauwens, W. (2011). Environmental Modelling & Software Sobol ' sensitivity analysis of a complex environmental model. *Environmental Modelling and Software*, *26*(12), 1515–1525. https://doi.org/10.1016/j.envsoft.2011.08.010

Part 630 Hydrology National Engineering Handbook Chapter 9. (2004).

Pfannerstill, M., Guse, B., Reusser, D., & Fohrer, N. (2015). *Process verification of a* *hydrological model using a temporal parameter sensitivity analysis*. 4365–4376. https://doi.org/10.5194/hess-19-4365-2015

Pianosi, F., Beven, K., Freer, J., Hall, J. W., Rougier, J., Stephenson, D. B., & Wagener, T. (2016). Environmental Modelling & Software Sensitivity analysis of environmental models : A systematic review with practical work fl ow. *Environmental Modelling and Software*, *79*, 214–232. https://doi.org/10.1016/j.envsoft.2016.02.008

Rai, P. K., Chahar, B. R., & Dhanya, C. T. (2017). GIS-based SWMM model for simulating the catchment response to flood events. *Hydrology Research*, *48*(2), 384–394. https://doi.org/10.2166/nh.2016.260

Renard, B., Kavetski, D., Kuczera, G., Thyer, M., & Franks, S. W. (2010). Understanding predictive uncertainty in hydrologic modeling: The challenge of identifying input and structural errors. *Water Resources Research*, *46*(5), 1–22. https://doi.org/10.1029/2009WR008328

Rossman, L.A. (2006). *Epa SWMM 5.0 Quality assurance report: Dynamic Wave Flow Routing*. *September*, 115.

Rossman, Lewis A. (2010). *SWMM 5.0 Users Manual.pdf*. *July*.

Rossman, Lewis A. (2015). Storm Water Management Model User'S Manuel 5.1. *Environ Prot Technol Ser EPA*, *September*.

Saltelli, A. (1999). Sensitivity analysis: Could better methods be used? *Journal of Geophysical Research Atmospheres*, *104*(D3), 3789–3793. https://doi.org/10.1029/1998JD100042

Saltelli, A. (2014). *Global sensitivity analysis : An introduction Global Sensitivity Analysis : An*

Introduction. *May*.

Saltelli, A., Annoni, P., Azzini, I., Campolongo, F., Ratto, M., & Tarantola, S. (2010). Variance based sensitivity analysis of model output. Design and estimator for the total sensitivity index. *Computer Physics Communications*, *181*(2), 259–270. https://doi.org/10.1016/j.cpc.2009.09.018

Saltelli, A., & Homma, T. (1996). Importance measures in global sensitivity analysis of model output. *Reliab. Eng. Sys. Safety*, *52*, 1–17.

Saltelli, A., Ratto, M., Andres, T., Campolongo, F., Cariboni, J., Gatelli, D., Saisana, M., & Tarantola. (2008). *Global sensitivity analysis: the primer*. https://doi.org/10.1002/9780470725184

Saltelli, A., Ratto, M., Tarantola, S., & Campolongo, F. (2012). Update 1 of: Sensitivity analysis for chemical models. *Chemical Reviews*, *112*(5). https://doi.org/10.1021/cr200301u

Saltelli, K. C. A., & Tarantola, S. (1997). *SENSITIVITY ANALYSIS OF MODEL OUTPUT: VARIANCE-BASED METHODS MAKE THE DIFFERENCE*. *1*, 261–268. https://doi.org/10.1109/WSC.1997.640407

Sanadhya, P., Gironás, J., & Arabi, M. (2014). *Global sensitivity analysis of hydrologic processes in major snow-dominated mountainous river basins in Colorado*. *3418*(June 2013), 3404–3418. https://doi.org/10.1002/hyp.9896

Shahed Behrouz, M., Zhu, Z., Matott, L. S., & Rabideau, A. J. (2020). A new tool for automatic calibration of the Storm Water Management Model (SWMM). *Journal of Hydrology*, *581*(February 2019), 124436. https://doi.org/10.1016/j.jhydrol.2019.124436

Shahed, M., Zhu, Z., Matott, L. S., & Rabideau, A. J. (2020). A new tool for automatic calibration of the Storm Water Management Model. *Journal of Hydrology*, *581*(December 2019), 124436. https://doi.org/10.1016/j.jhydrol.2019.124436

Shifflett, S. D., Newcomer-Johnson, T., Yess, T., & Jacobs, S. (2019). Interdisciplinary collaboration on green infrastructure for urbanwatershed management: An Ohio case study. *Water (Switzerland)*, *11*(4). https://doi.org/10.3390/w11040738

Singh, J., Knapp, H. V., Arnold, J. G., & Demissie, M. (2005). Hydrological modeling of the Iroquois River watershed using HSPF and SWAT. *Journal of the American Water Resources Association*, *41*(2), 343–360. https://doi.org/10.1111/j.1752-1688.2005.tb03740.x

Soil Survey Staff. (2019). *Web Soil Survey*. https://websoilsurvey.sc.egov.usda.gov/App/WebSoilSurvey.aspx

Song, X., Zhang, J., Zhan, C., Xuan, Y., Ye, M., & Xu, C. (2015). Global sensitivity analysis in hydrological modeling: Review of concepts, methods, theoretical framework, and applications. *Journal of Hydrology*, *523*(225), 739–757. https://doi.org/10.1016/j.jhydrol.2015.02.013

Suriya, S., & Mudgal, B. V. (2012). Impact of urbanization on flooding: The Thirusoolam sub watershed - A case study. *Journal of Hydrology*, *412–413*, 210–219. https://doi.org/10.1016/j.jhydrol.2011.05.008

Tasdighi, A., Arabi, M., & Harmel, D. (2018). A probabilistic appraisal of rainfall-runoff modeling approaches within SWAT in mixed land use watersheds. *Journal of Hydrology*, *564*(February), 476–489. https://doi.org/10.1016/j.jhydrol.2018.07.035

USDA-NRCS. (2010). *National Engineering Handbook Chapter 15, Time of Concentration*. 1–15.

Vogel, R. M., & Fennessey, N. M. (1996). FLOW DURATION CURVES II : A REVIEW OF APPLICATIONS IN WATER RESOURCES PLANNING ’ proverb " one picture is worth a thousand words " are used to summarize the results of detailed and ly , streamfiow duration curves have been used in sparse . This is the fir. *Water Resources Bulletin*, *31*(6), 1029–1039.

Vrugt, J. A. (2016). Markov chain Monte Carlo simulation using the DREAM software package: Theory, concepts, and MATLAB implementation. *Environmental Modelling and Software*, *75*, 273–316. https://doi.org/10.1016/j.envsoft.2015.08.013

Wagener, T. (2013). Technical note: Method of Morris effectively reduces the computational demands of global sensitivity analysis for distributed watershed models. *Hydrology and Earth System Sciences Discussions*, *10*(4), 4275–4299. https://doi.org/10.5194/hessd-10-4275-2013

Watson, M. (1996). City of Sacramento Stormwater Management Model (SSWMM96) User’s Manual. *Management*, *January*, 92.